25. Aboussekhra, A., Biggerstaff, M., Shivji, M.K., Vilpo, J.A., Moncollin, V., Podust, V.N., Protić, M., Hübscher, U., Egly, J.M., and Wood, R.D. (1995). Mammalian DNA nucleotide excision repair reconstituted with purified protein components. Cell *80*, 859–868.
26. Araújo, S.J., Nigg, E.A., and Wood, R.D. (2001). Strong functional interactions of TFIIH with XPC and XPG in human DNA nucleotide excision repair, without a preassembled repairosome. Mol. Cell. Biol. *21*, 2281–2291.
27. Kim, Y., Lach, F.P., Desetty, R., Hanenberg, H., Auerbach, A.D., and Smogorzewska, A. (2011). Mutations of the SLX4 gene in Fanconi anemia. Nat. Genet. *43*, 142–146.
28. Crossan, G.P., van der Weyden, L., Rosado, I.V., Langevin, F., Gaillard, P.H., McIntyre, R.E., Gallagher, F., Kettunen, M.I., Lewis, D.Y., Brindle, K., et al.; Sanger Mouse Genetics Project. (2011). Disruption of mouse Slx4, a regulator of structure-specific nucleases, phenocopies Fanconi anemia. Nat. Genet. *43*, 147–152.
29. Stoepker, C., Hain, K., Schuster, B., Hilhorst-Hofstee, Y., Rooimans, M.A., Steltenpool, J., Oostra, A.B., Eirich, K., Korthof, E.T., Nieuwint, A.W., et al. (2011). SLX4, a coordinator of structure-specific endonucleases, is mutated in a new Fanconi anemia subtype. Nat. Genet. *43*, 138–141.
30. de Laat, W.L., Appeldoorn, E., Jaspers, N.G., and Hoeijmakers, J.H. (1998). DNA structural elements required for ERCC1-XPF endonuclease activity. J. Biol. Chem. *273*, 7835–7842.
31. Tian, M., Shinkura, R., Shinkura, N., and Alt, F.W. (2004). Growth retardation, early death, and DNA repair defects in mice deficient for the nucleotide excision repair enzyme XPF. Mol. Cell. Biol. *24*, 1200–1205.
32. McWhir, J., Selfridge, J., Harrison, D.J., Squires, S., and Melton, D.W. (1993). Mice with DNA repair gene *(ERCC-1)* deficiency have elevated levels of p53, liver nuclear abnormalities and die before weaning. Nat. Genet. *5*, 217–224.
33. Weeda, G., Donker, I., de Wit, J., Morreau, H., Janssens, R., Vissers, C.J., Nigg, A., van Steeg, H., Bootsma, D., and Hoeijmakers, J.H.J. (1997). Disruption of mouse *ERCC1* results in a novel repair syndrome with growth failure, nuclear abnormalities and senescence. Curr. Biol. *7*, 427–439.
34. Kim, H., and D'Andrea, A.D. (2012). Regulation of DNA cross-link repair by the Fanconi anemia/BRCA pathway. Genes Dev. *26*, 1393–1408.
35. Garaycoechea, J.I., Crossan, G.P., Langevin, F., Daly, M., Arends, M.J., and Patel, K.J. (2012). Genotoxic consequences of endogenous aldehydes on mouse haematopoietic stem cell function. Nature *489*, 571–575.
36. Bogliolo, M., Schuster, B., Stoepker, C., Derkunt, B., Su, Y., Raams, A., Trujillo, J.P., Minguillón, J., Ramírez, M.J., Pujol, R., et al. (2013). Mutations in *ERCC4*, Encoding the DNA-Repair Endonuclease XPF, Cause Fanconi Anemia. Am. J. Hum. Genet. *92*. Published online April 25, 2013. http://dx.doi.org/10.1016/j.ajhg.2013.04.002.

RESEARCH ARTICLE

AMERICAN JOURNAL OF medical genetics PART A

MLL2 and *KDM6A* Mutations in Patients With Kabuki Syndrome

Noriko Miyake,[1]* Eriko Koshimizu,[1] Nobuhiko Okamoto,[2] Seiji Mizuno,[3] Tsutomu Ogata,[4] Toshiro Nagai,[5] Tomoki Kosho,[6] Hirofumi Ohashi,[7] Mitsuhiro Kato,[8] Goro Sasaki,[9] Hiroyo Mabe,[10] Yoriko Watanabe,[11] Makoto Yoshino,[11] Toyojiro Matsuishi,[11] Jun-ichi Takanashi,[12] Vorasuk Shotelersuk,[13] Mustafa Tekin,[14] Nobuhiko Ochi,[15] Masaya Kubota,[16] Naoko Ito,[17] Kenji Ihara,[17] Toshiro Hara,[17] Hidefumi Tonoki,[18] Tohru Ohta,[19] Kayoko Saito,[20] Mari Matsuo,[20] Mari Urano,[20] Takashi Enokizono,[21] Astushi Sato,[22] Hiroyuki Tanaka,[23] Atsushi Ogawa,[24] Takako Fujita,[25] Yoko Hiraki,[26] Sachiko Kitanaka,[22] Yoichi Matsubara,[27] Toshio Makita,[28] Masataka Taguri,[29] Mitsuko Nakashima,[1] Yoshinori Tsurusaki,[1] Hirotomo Saitsu,[1] Ko-ichiro Yoshiura,[30] Naomichi Matsumoto,[1]* and Norio Niikawa[19]

[1]Department of Human Genetics, Yokohama City University Graduate School of Medicine, Yokohama, Japan

[2]Department of Medical Genetics, Osaka Medical Center and Research Institute for Maternal and Child Health, Izumi, Japan

[3]Department of Pediatrics, Central Hospital, Aichi Human Service Center, Kasugai, Japan

[4]Department of Pediatrics, Hamamatsu University School of Medicine, Hamamatsu, Japan

[5]Department of Pediatrics, Dokkyo Medical University Koshigaya Hospital, Saitama, Japan

[6]Department of Medical Genetics, Shinshu University School of Medicine, Matsumoto, Japan

[7]Division of Medical Genetics, Saitama Children's Medical Center, Iwatsuki, Japan

[8]Department of Pediatrics, Yamagata University Faculty of Medicine, Yamagata, Japan

[9]Department of Pediatrics, Tokyo Dental College Ichikawa General Hospital, Chiba, Japan

[10]Department of Child Development, Kumamoto University Hospital, Kumamoto, Japan

[11]Department of Pediatrics and Child Health, Kurume University School of Medicine, Kurume, Japan

[12]Department of Pediatrics, Kameda Medical Center, Kamogawa, Chiba, Japan

[13]Center of Excellence for Medical Genetics, Department of Pediatrics, Faculty of Medicine, Chulalongkorn University, Bangkok, Thailand

[14]John P. Hussman Institute for Human Genomics, Miller School of Medicine, University of Miami, Miami, Florida

[15]Department of Pediatrics, Aichi Prefectural Hospital and Habilitation Center for Disabled Children, Dai-ni Aoitori Gakuen, Okazaki, Japan

[16]Division of Neurology, National Center for Child Health and Development, Tokyo, Japan

[17]Department of Pediatrics, Graduate School of Medical Sciences, Kyushu University, Fukuoka, Japan

[18]Section of Clinical Genetics, Department of Pediatrics, Tenshi Hospital, Sapporo, Japan

[19]Research Institute of Personalized Health Sciences, Health Science University of Hokkaido, Tobetsu, Japan

[20]Institute of Medical Genetics, Tokyo Women's Medical University, Tokyo, Japan

[21]Department of Pediatrics, University of Tsukuba Hospital, Tsukuba, Japan

[22]Department of Pediatrics, Graduate School of Medicine, The University of Tokyo, Tokyo, Japan

[23]Department of Pediatrics, Ohta Nishinouchi Hospital, Tokyo, Japan

[24]Department of Pediatrics, Chikushi Hospital, Fukuoka University, Fukuoka, Japan

[25]Department of Pediatrics, Fukuoka University School of Medicine, Fukuoka, Japan

[26]Hiroshima Municipal Center for Child Health and Development, Hiroshima, Japan

[27]Department of Medical Genetics, Tohoku University School of Medicine, Sendai, Japan

[28]Education Center, Asahikawa Medical University, Asahikawa, Japan

[29]Department of Biostatistics and Epidemiology, Yokohama City University Graduate School of Medicine, Yokohama, Japan

[30]Department of Human Genetics, Graduate School of Biomedical Sciences, Nagasaki University, Nagasaki, Japan

Manuscript Received: 9 January 2013; Manuscript Accepted: 9 May 2013

Kabuki syndrome is a congenital anomaly syndrome characterized by developmental delay, intellectual disability, specific facial features including long palpebral fissures and ectropion of the lateral third of the lower eyelids, prominent digit pads, and skeletal and visceral abnormalities. Mutations in *MLL2* and *KDM6A* cause Kabuki syndrome. We screened 81 individuals with Kabuki syndrome for mutations in these genes by conventional methods (n = 58) and/or targeted resequencing (n = 45) or whole exome sequencing (n = 5). We identified a mutation in *MLL2* or *KDM6A* in 50 (61.7%) and 5 (6.2%) cases, respectively. Thirty-five *MLL2* mutations and two *KDM6A* mutations were novel. Non-protein truncating-type *MLL2* mutations were mainly located around functional domains, while truncating-type mutations were scattered through the entire coding region. The facial features of patients in the *MLL2* truncating-type mutation group were typical based on those of the 10 originally reported patients with Kabuki syndrome; those of the other groups were less typical. High arched eyebrows, short fifth finger, and hypotonia in infancy were more frequent in the *MLL2* mutation group than in the *KDM6A* mutation group. Short stature and postnatal growth retardation were observed in all individuals with *KDM6A* mutations, but in only half of the group with *MLL2* mutations. © 2013 Wiley Periodicals, Inc.

Key words: Kabuki syndrome; *MLL2*; *KDM6A*; mutation; genotype–phenotype correlation

How to Cite this Article:
Miyake N, Koshimizu E, Okamoto N, Mizuno S, Ogata T, Nagai T, Kosho T, Ohashi H, Kato M, Sasaki G, Mabe H, Watanabe Y, Yoshino M, Matsuishi T, Takanashi J-i, Shotelersuk V, Tekin M, Ochi N, Kubota M, Ito N, Ihara K, Hara T, Tonoki H, Ohta T, Saito K, Matsuo M, Urano M, Enokizono T, Sato A, Tanaka H, Ogawa A, Fujita T, Hiraki Y, Kitanaka S, Matsubara Y, Makita T, Taguri M, Nakashima M, Tsurusaki Y, Saitsu H, Yoshiura K-i, Matsumoto N, Niikawa N. 2013. *MLL2* and *KDM6A* mutations in patients with Kabuki syndrome.
Am J Med Genet Part A 161A:2234–2243.

INTRODUCTION

Kabuki syndrome (KS; OMIM 147920) is a multiple congenital anomaly syndrome that was originally reported by Niikawa et al. [1981] and Kuroki et al. [1981] (also known as Kabuki make-up syndrome or Niikawa–Kuroki syndrome). KS is diagnosed clinically by characteristic facial features, including long palpebral fissures and ectropion of the lateral third of the lower eyelids, postnatal growth impairment (short stature), developmental delay, intellectual disability, dermatoglyphic abnormalities, visceral and skeletal abnormalities, and immunological dysfunction. The prevalence of the disorder is estimated to be 1 in 32,000 live births [Niikawa et al., 1988]. Two genes have shown to be mutated in patients with KS: *MLL2* (myeloid/lymphoid or mixed-lineage leukemia 2; NM_003482.3) at 12q13.12 and *KDM6A* (lysine (K)-specific demethylase 6A; NM_021140.2) at Xp11.3 [Ng et al., 2010; Lederer et al., 2012; Miyake et al., 2013]. *MLL2* encodes a histone H3 lysine 4 (H3K4)-specific methyl transferase and KDM6A is a specific demethylase of histone H3 lysine 27 (H3K27) [Prasad et al., 1997; Lee et al., 2007]. They are both trithorax group proteins and bind each other [Schuettengruber et al., 2007]. These proteins are important for the chromatin state and transcription activation: MLL2 methylates H3K4 and KMD6A removes the H3K27 trimethylation repressive mark [Dubuc et al., 2013]. The loss of MLL2 or KDM6A function may lead to repressed transcription [Dubuc et al., 2013].

To our knowledge, there has been no comprehensive screen for mutations in these two genes in the same patient series. In this report, we performed a mutation screen of both genes in 81 patients with KS. We then evaluated the clinical features based on the genetic information.

MATERIALS AND METHODS

Samples

Eighty-one individuals clinically suspected to have KS were incorporated in this study: 77 Japanese, two Caucasians, one Belgian, and one Thai. They were all sporadic except for KMS-79, who had an affected sibling. Peripheral blood samples or saliva samples from the

Additional supporting information may be found in the online version of this article at the publisher's web-site.

Conflict of interest: none.
Grant sponsor: Ministry of Health, Labour and Welfare of Japan; Grant sponsor: Japan Science and Technology Agency; Grant sponsor: Strategic Research Program for Brain Sciences; Grant sponsor: Ministry of Education, Culture, Sports, Science and Technology of Japan; Grant sponsor: Grant-in-Aid for Scientific Research from the Japan Society for the Promotion of Science; Grant sponsor: Grant-in-Aid for Young Scientists from the Japan Society for the Promotion of Science; Grant sponsor: Takeda Science Foundation; Grant sponsor: Yokohama Foundation for the Advancement of Medical Science; Grant sponsor: Hayashi Memorial Foundation for Female Natural Scientists.

*Correspondence to:
Dr. Noriko Miyake or Prof. Naomichi Matsumoto, Department of Human Genetics, Yokohama City University Graduate School of Medicine, 3-9 Fukuura, Kanazawa-ku, Yokohama 236-0004, Japan.
E-mails: nmiyake@yokohama-cu.ac.jp (N. Miyake) or naomat@yokohama-cu.ac.jp (N. Matsumoto)

Article first published online in Wiley Online Library (wileyonlinelibrary.com): 2 August 2013
DOI 10.1002/ajmg.a.36072

patients and their parents (when available) were collected with informed consent and DNA was extracted using a QuickGene-610L (Fujifilm, Tokyo, Japan) or Oragene-DNA kit (DNA Genotek, Inc., Ottawa, Canada) according to the manufacturer's instructions. This study included four previously reported patients (KMS-50, KMS-51, KMS-61, and KMS-71) [Tekin et al., 2006; Torii et al., 2009; Ito et al., 2012]. In addition, three patients with a *KDM6A* mutation were previously described as Patients 1, 2, and 3 by Miyake et al. [2013], and are named KMS-31, KMS-37, and KMS-65, respectively, in this report. This study was approved by the Institutional Review Board of Yokohama City University School of Medicine.

Mutation Screening

Fifty-eight patients (KMS-01 to KMS-69) were screened for *MLL2* mutations by the high-resolution melting (HRM) method using a LightCycler 480 System II (Roche Diagnostics, Indianapolis, IN) and subsequent Sanger sequencing. If an HRM curve pattern was different from those of controls, the DNA sample was Sanger sequenced on an ABI 3500xl or 3130xl Genetic Analyzer (Applied Biosystems, Foster City, CA) and the sequences were analyzed using Sequencher software version 4.10.1 (Gene Codes Corporation, Ann Arbor, MI). *KDM6A* was analyzed in samples with no *MLL2* mutation using HRM analysis and Sanger sequencing as above (n = 37). For male samples, genotyping using spike-in control male genomic DNA (10%) was performed to detect a hemizygous mutation. The latter 23 patients (KMS-70 to KMS-92), as well as 22 patients with no mutation in either gene detected by conventional methods, were analyzed by targeted resequencing as described in the following section. We judged a variant as pathogenic when it was previously reported to cause KS, or novel variant when it was not observed in unaffected parents or in in-house exome data (n = 977), dbSNP135, or EVS6500 (Exome Variant Server, NHLBI GO Exome Sequencing Project, Seattle, WA; http://evs.gs.washington.edu/EVS/; accessed March 1, 2013). In addition, the missense mutation predicted to be polymorphism by both of two predictions (Polyphen-2: http://genetics.bwh.harvard.edu/pph2/ [Adzhubei et al., 2010] and MutationTaster: http://www.mutationtaster.org/ [Schwarz et al., 2010]) was considered to be non-pathogenic. Parentage analysis was conducted for the patients only when the parental samples were available. TaKaRa Ex Taq and TaKaRa LA Taq (both Takara, Tokyo, Japan) were used for amplification. The primer sequences and PCR conditions are available on request. All pathological variants were confirmed by Sanger sequencing. Nucleotide numbering reflects cDNA numbering with +1 corresponding to the A of the ATG translation initiation codon in the reference sequence (RefSeq NM_003482.3 for *MLL2*, RefSeq NM_021140.2 for *KDM6A*).

Targeted Resequencing of *MLL2* and *KDM6A* by Next-Generation Sequencing

Ion AmpliSeq Custom Panels (Life Technologies, Inc., Grand Island, NY) covering the entire coding region of *MLL2* and *KDM6A* were created via the Ion AmpliSeq Designer v1.2 (https://ampliseq.com/browse.action). Libraries were prepared using the Ion AmpliSeq Library Kit 2.0 (Life Technologies, Inc.), with 10 ng of genomic DNA for each primer pool (two pools for this analysis). An Agilent 2200 TapeStation (Agilent Technologies, Santa Clara, CA) and the associated High Sensitivity D1K Screen Tape (Agilent Technologies) were used to check the size distribution and the concentration of the DNA libraries. Emulsion PCR and enrichment steps were carried out using the Ion OneTouch 200 Template Kit v2 (Life Technologies, Inc.). The amplicon libraries were sequenced on an Ion Torrent Personal Genome Machine system using 314 or 316 chips, and bar-coding was applied with an Ion Xpress Barcode Adapters 1–16 Kit (all Life Technologies, Inc.). Torrent Suite 2.2 (Life Technologies, Inc.) was used for mapping, base calling, and variant calling. Sequences were annotated using SeattleSeq Annotation 134 (http://snp.gs.washington.edu/SeattleSeqAnnotation134/). All variants were confirmed by Sanger sequencing.

Whole Exome Sequencing by High-Throughput Next-Generation Sequencing

Whole exome sequencing was performed in five individuals (KMS-09, -18, -21, -23, and -61) who had no *MLL2* or *KDM6A* abnormality by HRM analysis. DNA was processed with a SureSelect Human All Exon V4 kit (Agilent Technologies), sequenced on a HiSeq2000 (Illumina, Inc., San Diego, CA), and analyzed as previously described [Tsurusaki et al., 2013]. Variants in *MLL2* and *KDM6A* were confirmed by Sanger sequencing.

X-Inactivation Assay

X-inactivation analysis was performed as described [Allen et al., 1992] with slight modification. Briefly, genomic DNA (500 ng) was digested with two methylation-sensitive restriction enzymes, *Hpa*II and *Hha*I (New England Biolabs, Beverly, MA), and purified by phenol/chloroform extraction and ethanol precipitation. Digested and undigested DNA samples (10 ng) were separately amplified for the (CAG)*n* polymorphism at the androgen receptor locus. The forward primer was labeled with 5′ FAM dye. PCR products were analyzed on an ABI 3500xl Genetic Analyzer using GeneMapper Software Version 4.1 (Applied Biosystems). The assay was independently performed twice.

cDNA Sequencing

Total RNA was extracted from a lymphoblastoid cell line established from KMS-81 (c.1909_1912del in *KDM6A*) using an RNeasy Plus mini kit (Qiagen, Hilden, Germany) with and without cycloheximide treatment (30 μg/ml) for 4 hr before cell collection. Reverse transcription (RT) was performed using a Superscript III First-Strand synthesis system for RT-PCR (Life Technologies, Inc.). As the mutation was located in exon 17, the region from the exon 15/16 boundary to the exon 17/18 boundary of *KDM6A* was amplified using cDNA-specific primer pairs (sequences available on request) and sequenced by the Sanger method.

Statistical Analysis

The frequencies of clinical features in the two groups were compared by Fisher's exact test. A difference was considered statistically

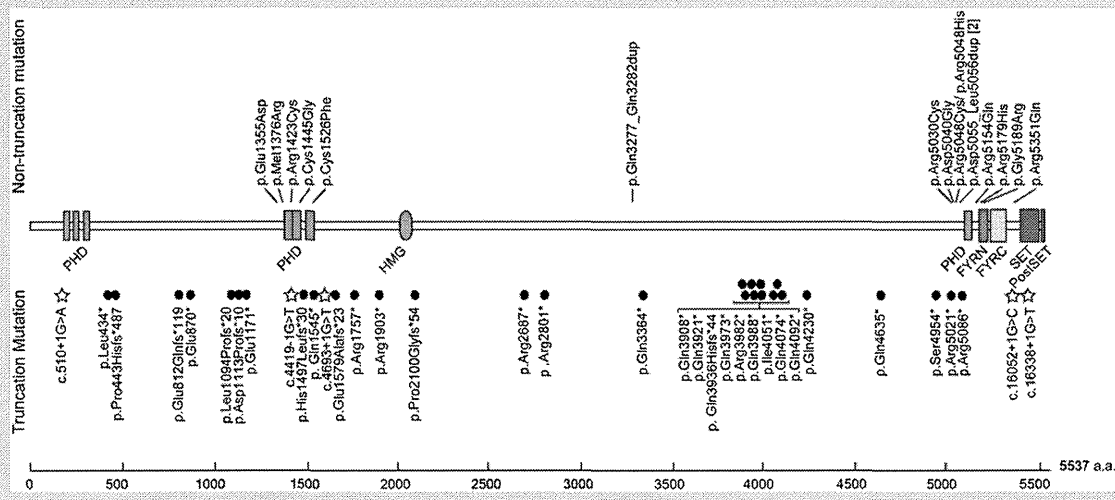

FIG. 1. *MLL2* mutations in patients with Kabuki syndrome. Upper: Non-truncating-type mutations. Middle: MLL2 protein structure with functional domains. The protein contains seven plant homeodomains (PHD), one high-mobility group (HMG) domain, a Phe-Tyr-rich *N*-terminal (FYRN) domain, a Phe-Tyr-rich *C*-terminal (FYRC) domain, a SET (Suvar3-9, Enhancer-of-zeste, Trithorax) domain, and a PostSET domain. These functional domains were based on a prediction by SMART (http://smart.embl-heidelberg.de/) and the UniProtKB database (http://www.uniprot.org/uniprot/O14686). Lower: Truncating-type mutations. Black circles denote nonsense mutations or frameshift mutations. Stars represent splice-site mutations.

significant if $P < 0.05$. Correction for multiple testing was not applied.

RESULTS

Overall Mutation Detection Rates

Pathogenic mutations in *MLL2* and *KDM6A* were found in 50 (61.7%) and five (6.2%) of the 81 patients with KS, respectively (Figs. 1 and 2, Tables I and II). Of the 50 *MLL2* mutations, 35 (70.0%) were predicted to be protein truncating-type and 15 (30.0%) were predicted to be non-truncating-type. Interestingly, non-truncating mutations were mostly localized in or adjacent to the functional domains, while truncating mutations were scattered throughout the entire coding region (Fig. 1). Fifteen of the *MLL2* mutations have been previously reported (Table I). Three novel variants (not included in the 50 mutations) were considered non-pathogenic (Supplemental Table I). Variant c.10942C > G in patient KMS-22 was predicted to be benign by Polyphen-2 and MutationTaster, c.8813C > T in patient KMS-62 was inherited from an unaffected father, and c.4065A > T in KMS-75 was found heterozygously in our 977 in-house controls. An in-frame duplication in patients KMS-40 and KMS-62, which predicted p.Asp5055_Leu5056dup, was predicted to be polymorphic by MutationTaster, but was previously reported as a pathogenic mutation [Micale et al., 2011]. In addition, the other in-frame mutation in KMS-02 was also predicted to be polymorphic. Unfortunately, parental samples were unavailable for these individuals, except for the mother of patient KMS-62, who did not have this mutation; thus, the de novo status remains unclear. Of the five *KDM6A* mutations including three mutations reported previously [Miyake et al., 2013], four were truncating-type and one was an in-frame deletion located within the Jumonji C domain (Fig. 2).

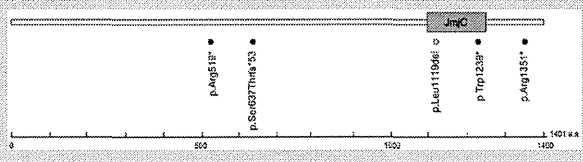

FIG. 2. *KDM6A* mutations in patients with Kabuki syndrome. Upper: Scheme of KDM6A protein. It contains a Jumonji C (JmjC) domain (purple box). Lower: Black circles indicate truncating-type mutations (nonsense or frameshift mutations); the white circle represents a non-truncating-type mutation (in-frame deletion).

Clinical Comparison Between the Mutation-Positive and -Negative Groups

We compared the clinical features of the *MLL2* or *KDM6A* mutation-positive and -negative groups (Supplemental Table II). Long palpebral fissures were observed in almost all patients. Cleft lip/palate was more frequently observed in the mutation-positive group ($P = 0.0197$). Interestingly, developmental delay and intellectual disability were observed in all individuals with mutations but were unobserved in some mutation-negative cases ($P = 0.0314$

TABLE I. *MLL2* and *KDM6A* Mutations in Patients With KS

Patient ID	Method	Mutation	Predicted amino acid change	De novo	Remarks[a]
Patients with *MLL2* mutations					
KMS-02	H	c.9831_9848dup	p.Gln3277_Gln3282dup	Unknown	Novel
KMS-08	H	c.12688C > T	p.Gln4230*	Yes	Hannibal et al. [2011]
KMS-13	H	c.2433_2434insCA	p.Glu812Glnfs*119	Yes	Novel
KMS-14	H	c.11806_11807dup	p. Gln3936Hisfs*44	Yes	Novel
KMS-15	H	c.15119A > G	p.Asp5040Gly	Yes	Novel
KMS-17	H	c.5707C > T	p.Arg1903*	Yes	Novel
KMS-18	W	c.12151delA	p.Ile4051*	Yes	Novel
KMS-20	H	c.1300delC	p.Leu434*	Unknown	Novel
KMS-21	W	c.3326_3336dup	p.Asp1113Profs*10	Unknown	Novel
KMS-22	H	c.4127T > G	p.Met1376Arg	Unknown	Novel
KMS-23	W	c.15461G > A	p.Arg5154Gln	Unknown	Li et al. [2011]
KMS-24	H	c.2608 G > T	p.Glu870*	Unknown	Novel
KMS-25	H	c.11917C > T	p.Gln3973*	Unknown	Novel
KMS-27	H	c.15142C > T	p.Arg5048Cys	Yes	Hannibal et al. [2011], Makrythanasis et al. [2013]
KMS-28	H	c.14861C > A	p.Ser4954*	Unknown	Novel
KMS-29	H	c.4419-1G > T	splice site	Unknown	Novel
KMS-30	H	c.4633C > T	p. Gln1545*	Unknown	Novel
KMS-32	H	c.8059C > T	p.Arg2687*	Unknown	Banka et al. [2012b]
KMS-33	T	c.11962C > T	p.Gln3988*	Unknown	Novel
KMS-36	H	c.4736_4737delAG	p.Glu1579Alafs*23	Unknown	Novel
KMS-38	H	c.15143G > A	p.Arg5048His	Unknown	Makrythanasis et al. [2013]
KMS-40	T	c.15163_15168dup	p.Asp5055_Leu5056dup	Unknown	Micale et al. [2011]
KMS-41	H	c.1328delC	p.Pro443Hisfs*487	Yes	Ng et al. [2010]
KMS-42	H	c.16052G > A	p.Arg5351Gln	Yes	Novel
KMS-43	H	c.510 + 1G > A	splice site	Unknown	Novel
KMS-49	T	c.15565G > A	p.Gly5189Arg	Unknown	Novel
KMS-51[b]	H	c.6297_6298delAC	p.Pro2100Glyfs*54	Yes	Novel
KMS-52	H	c.4693 + 1G > T	splice site	Yes	Novel
KMS-53	H	c.10090C > T	p.Gln3364*	Yes	Novel
KMS-54	T	c.8401C > T	p.Arg2801*	Yes	Novel
KMS-56	H	c.15536G > A	p.Arg5179His	Yes	Ng et al. [2010]
KMS-58	H	c.4333T > G	p.Cys1445Gly	Yes	Novel
KMS-59	H	c.15256C > T	p.Arg5086*	Yes	Banka et al. [2012b]
KMS-60	H	c.11761C > T	p.Gln3921*	Unknown	Novel
KMS-61[c]	W	c.5269C > T	p.Arg1757*	Yes	Novel
KMS-62	H	c.15163_15168dup	p.Asp5055_Leu5056dup	Unknown[f]	Micale et al. [2011]
KMS-63	T	c.4577G > T	p.Cys1526Phe	Yes	Novel
KMS-69	H	c.11944C > T	p.Arg3982*	Yes	Paulussen et al. [2011]
KMS-70	T	c.13903C > T	p.Gln4635*	Yes	Novel
KMS-71[d]	T	c.12220C > T	p.Gln4074*	Unknown	Novel
KMS-72	T	c.15061C > T	p.Arg5021*	Yes	Banka et al. [2012b]
KMS-73	T	c.12274C > T	p.Gln4092*	Unknown	Micale et al. [2011]
KMS-76	T	c.4490_4491delAC	p.His1497Leufs*30	Yes	Novel
KMS-78	T	c.16338 + 1G > T	splice site	Yes	Novel
KMS-80	T	c.15088C > T	p.Arg5030Cys	Unknown	Makrythanasis et al. [2013]
KMS-82	T	c.3511G > T	p.Glu1171*	Yes	Novel
KMS-85	T	c.11722C > T	p.Gln3908*	Yes	Paulussen et al. [2011]
KMS-87	T	c.3281_3282delTC	p.Leu1094Profs*20	Yes	Novel
KMS-88	T	c.16052 + 1G > C	splice site	Unknown	Novel
KMS-91	T	c.4267C > T	p.Arg1423Cys	Unknown	Novel
Patients with *KDM6A* mutations					
KMS-31[e]	H	c.3717G > A	p.Trp1239*	Unknown	Miyake et al. [2013]
KMS-37[e]	H	c.1555C > T	p.Arg519*	Unknown	Miyake et al. [2013]
KMS-65[e]	H	c.3354_3356delTCT	p.Leu1119del	Yes	Miyake et al. [2013]
KMS-81	T	c.1909_1912delTCTA	p.Ser637Thrfs*53	Yes	Novel
KMS-83	T	c.4051C > T	p.Arg1351*	Unknown	Novel

H, high-resolution melting analysis/Sanger sequencing; T, targeted resequencing; W, whole exome sequencing.RefSeq NM_003482.3 for *MLL2* and RefSeq NM_021140.2 for *KDM6A* were used as reference sequences.

[a]References are listed when the same mutation has been reported previously.

[b]This patient was reported as proband 1 by Tekin et al. [2006].

[c]The detailed clinical features of this patient were reported by Ito et al. [2013] because of her hypothalamic pituitary complications.

[d]The clinical course of this patient, particularly the idiopathic thrombocytopenic purpura, was reported by Torii et al. [2009].

[e]These patients have been reported in our previous study [Miyake et al., 2013].

[f]Patient KMS-62: no mutation in the mother.

TABLE II. *MLL2* Non-Truncating-Type Mutations in Patients With KS

Amino acid change[a]	Patient ID	Domain	Polyphen-2 (score)	MutationTaster
p.Met1376Arg	KMS-22	—	Probably damaging (0.915)	Polymorphism
p.Arg1423Cys	KMS-91	PHD	Probably damaging (1.000)	Disease causing
p.Cys1445Gly	KMS-58	PHD	Probably damaging (1.000)	Disease causing
p.Cys1526Phe	KMS-63	PHD	Probably damaging (0.999)	Disease causing
p.Gln3277_Gln3282dup	KMS-02	—	NA	Polymorphism
p.Arg5030Cys	KMS-80	—	Probably damaging (1.000)	Disease causing
p.Asp5040Gly	KMS-15	—	Probably damaging (1.000)	Disease causing
p.Arg5048Cys	KMS-27	—	Probably damaging (1.000)	Disease causing
p.Arg5048His	KMS-38	—	Probably damaging (1.000)	Disease causing
p.Asp5055_Leu5056dup	KMS-40, 62	—	NA	Polymorphism
p.Arg5154Gln	KMS-23	—	Probably damaging (1.000)	Disease causing
p.Arg5179His	KMS-56	FYRN	Possibly damaging (0.840)	Disease causing
p.Gly5189Arg	KMS-49	FYRN	Probably damaging (1.000)	Disease causing
p.Arg5351Gln	KMS-42	—	Probably damaging (1.000)	Disease causing

[a]The nucleotide mutation nomenclature for these predicted protein mutations are included in Table I.

and $P = 0.1778$, respectively). Blue sclera, lower lip pits, spine/rib abnormality, hip joint dislocation, umbilical hernia, kidney dysfunction, cryptorchidism, liver abnormality, spleen abnormality, premature thelarche, neonatal hyperbilirubinemia, and anemia were observed only in the mutation-positive group.

Clinical Comparison of the *MLL2*-Mutated and *KDM6A*-Mutated Groups

We compared the clinical features between the *MLL2*-mutated and *KDM6A*-mutated groups (Figs. 3–5, Supplemental Table III). High arched eyebrows, short fifth fingers, and hypotonia in infancy were more frequent in individuals with *MLL2* mutations than in individuals with *KDM6A* mutations ($P = 0.0364$, 0.0039, and 0.0283, respectively). Short stature was more frequent in individuals with *KDM6A* mutations ($P = 0.0485$). Although not statistically significant, postnatal growth retardation was observed in all individuals with *KDM6A* mutations, whereas this was observed in only half of the individuals with *MLL2* mutations.

Clinical Comparison of Individuals With a *MLL2* Truncating-Type and Non-Truncating-Type Mutation

Most clinical features were observed at a similar ratio in both groups (Supplemental Table IV), except for prominent ears and hypotonia, which were more frequently observed in the truncating-type group than in the non-truncating-type group ($P = 0.0339$ and $P = 0.0248$, respectively). However, the facial appearance of individuals in the truncating-type group was more typical, based on the ten originally reported patients with KS [Kuroki et al., 1981; Niikawa et al., 1981], than that in the non-truncating-type group (Figs. 3 and 4). Except for patient KMS-58, the facial appearance of patients with a non-truncating-type mutation was rather less typical. It should be noted that these patients had thick eyebrows (not present in patient KMS-56). Furthermore, ectropion of the lower eyelid, depressed nasal tip, short columella, and prominent ears all seemed less obvious in the individuals with a non-truncating-type mutation.

X-Inactivation Pattern in Female Patients With a *KDM6A* Mutation

A *KDM6A* mutation was identified in two females (KMS-65 and KMS-81). Individual KMS-65 (c.3354_3356del, which predicts p.Leu1119del) showed a random X-inactivation pattern [Miyake et al., 2013], while individual KMS-81 with a frame-shift mutation showed marked skewing (98:2; Supplemental Fig. 1A). By RT-PCR using mRNA derived from a lymphoblastoid cell line from patient KMS-81, we confirmed that both the mutated and normal alleles were transcribed at similar levels when nonsense-mediated mRNA decay (NMD) was inhibited by cycloheximide treatment (Supplemental Fig. 1B). In untreated cells, or cells treated with dimethylsulfoxide (negative control), the mutant allele was transcribed at a lower level than the wild-type allele, indicating that NMD partially eliminated the mutant.

Exome Sequencing

Among the five patients who were also analyzed by whole exome sequencing, mutations were identified and later confirmed by Sanger sequencing in four (Table I). Fragments with an 11 base-pair insertion (c.3326_3336dup) of *MLL2* in patient KMS-21 could not be amplified by Ex Taq, but could be amplified by LA Taq with LA buffer and confirmed by Sanger sequencing. Three other mutations were missed by HRM analysis (Table I).

DISCUSSION

We identified 50 *MLL2* and five *KDM6A* mutations among 81 patients with KS and add to the 246 *MLL2* mutations described in patients with KS [Ng et al., 2010; Hannibal et al., 2011; Li et al., 2011; Micale et al., 2011; Paulussen et al., 2011; Banka et al., 2012a,b;

FIG. 3. Clinical features of patients with Kabuki syndrome harboring a MLL2 truncating-type mutation. A: Facial features of patients with Kabuki syndrome with a *MLL2* truncating-type mutation. The seven panels for patient KMS-54 show serial images at 0, 1, 4, 6.5, 9.5, 22, and 33 years of age, respectively. B: Complete right cleft lip/palate and lower lip pits (arrows) in patient KMS-41. C: Abnormal dentition in patients KMS-52 and KMS-59. They also showed hypodontia with wide interdentium. D: Patient KMS-72 had congenital strabismus and blepharoptosis as well as opacification of the cornea due to Peters anomaly (arrow). E: Hand images show short fifth fingers and prominent digit pads (white arrows).

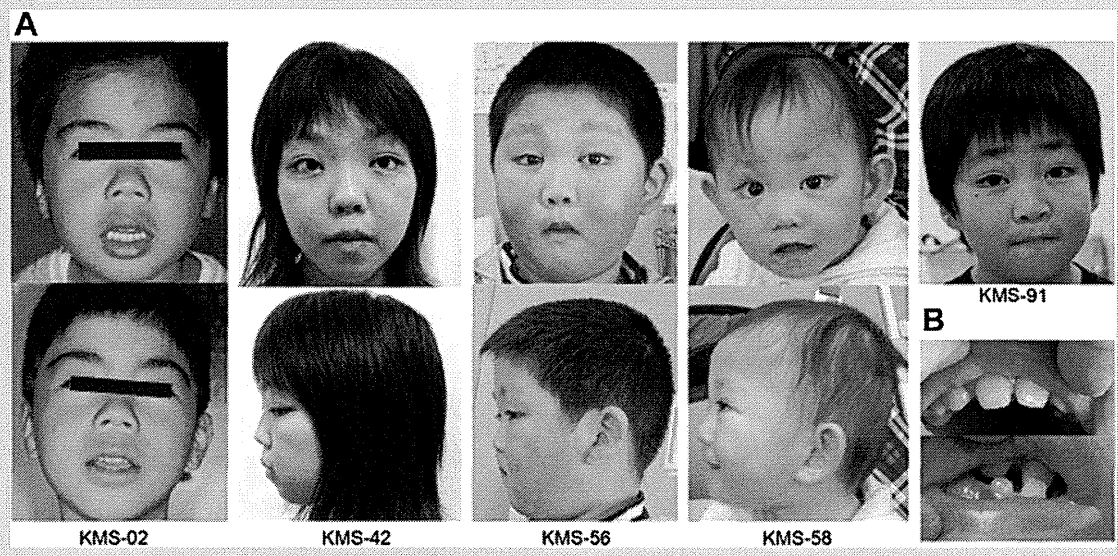

FIG. 4. Clinical features of patients with Kabuki syndrome with a *MLL2* non-truncating-type mutation. A: Facial features of patients with KS and a *MLL2* non-truncating-type mutation. B: Patient KMS-56 showed abnormal dentition (hypodontia with wide interdentium).

Kokitsu-Nakata et al., 2012; Tanaka et al., 2012; Bogershausen and Wollnik, 2013; Makrythanasis et al., 2013] (Human Gene Mutation Database Professional 2012.3; https://portal.biobase-international.com/hgmd/pro/gene.php). Our mutation-positivity rate for either gene was 67.9% (55/81), and that for *MLL2* only was 61.7% (50/81); these figures are compatible with those reported in a review (55–80%) [Banka et al., 2012b]. Mutation-negative patients suggest the existence of unknown genes to cause KS or misdiagnosis.

As for the phenotype–genotype relationship, Banka et al. [2012b] suggested that feeding problems, kidney anomalies, premature thelarche, joint dislocation, and palatal malformation were more frequently observed in patients with *MLL2*-mutations than in patients with normal *MLL2* sequence. Hannibal et al. [2011] reported that renal anomalies were more common in patients who had *MLL2* mutations compared to those who did not. Li et al. [2011] reported that short stature and renal anomalies were more frequent in patients with *MLL2*-mutations than in those with normal *MLL2* sequence. In our study, premature thelarche was observed only in patients with *MLL2* mutations, but this was not significant ($P = 0.1137$). The frequencies of kidney anomalies, hip joint dislocation, and short stature were not different when comparing those with and without *MLL2* mutations ($P = 0.3030$, $P = 1.0000$, and $P = 0.0717$, respectively; Supplemental Table V). High arched eyebrows, palatal malformation (cleft palate/lip), low posterior hairline, and short fifth finger were more frequently observed in individuals with *MLL2* mutations than in patients with normal *MLL2* ($P = 0.0118$, $P = 0.0284$, $P = 0.0493$, and $P = 0.0137$, respectively; Supplemental Table V).

X-inactivation skewing in patients with KS has been discussed since the discovery of the *KDM6A* deletion in a female with KS

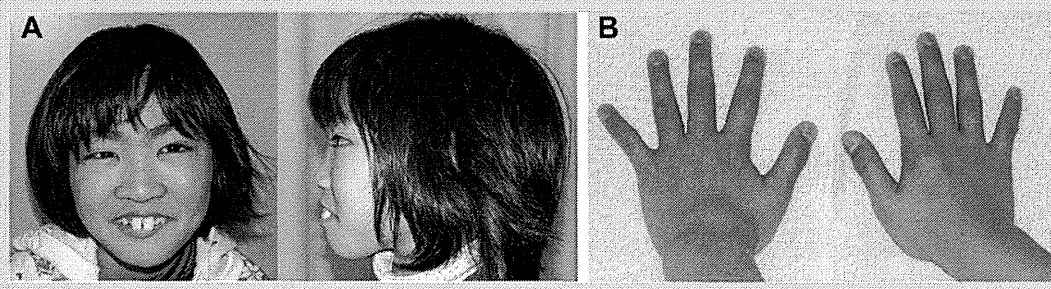

FIG. 5. Clinical features of patients with Kabuki syndrome with a *KDM6A* truncating-type mutation. A: Facial features of patient KMS-81 harboring a *KDM6A* mutation (c.1909_1912del, p.Ser637Thrfs*53). She showed large front teeth with wide interdentium. B: Hand image of KMS-81. Short fifth finger was not remarkable.

[Lederer et al., 2012; Miyake et al., 2013]. In two female patients reported here, patient KMS-65, who had an in-frame deletion, showed a random X-inactivation pattern, but patient KMS-81, who had a truncating-type mutation, showed marked skewing. X-inactivation skewing was also reported in two affected females with *KDM6A* deletion reported by Lederer et al. [2012]. cDNA sequence analysis of patient KMS-81 indicated that the mutant allele of *KDM6A* was expressed at a similar level to the wild-type allele under NMD inhibition. This result suggests that *KDM6A* mostly escapes X-inactivation in female lymphoblastoid cells. Interestingly, *KDM6A*/*Kdm6a* escapes X-inactivation in humans and mice, and in mice its expression level from the inactive X chromosome (Xi) was reported as 15–35% of that from the active X chromosome (Xa) [Greenfield et al., 1998; Xu et al., 2008]. We calculated the hypothetical expression assuming a 30% *KDM6A* expression level from Xi and 100% expression from Xa (Supplemental Fig. 2). In patient KMS-81, who showed marked skewing (98:2), either the mutant X chromosome or the wild-type X was inactivated in 98% of cells. If the mutant were inactivated, the expression level would be below 1 ($1.0 \times 0.98 + 0.3 \times 0.02 = 0.986$). If the wild-type were inactivated, the expression level would also be below 1 ($1.0 \times 0.02 + 0.3 \times 0.98 = 0.314$). The KS phenotype is usually unassociated with Turner syndrome (45,X), with the *KDM6A* expression level at 1.0 [Miyake et al., 2013]. It is possible that having a *KDM6A* expression level of 1.0 is essential for a normal human phenotype. Similarly, males with only one copy of *KDM6A* do not manifest KS. We previously mentioned the possibility of *UTY* compensation for *KMD6A* (Supplemental Fig. 2) [Miyake et al., 2013], although human UTY lacks demethylase activity [Hong et al., 2007; Lan et al., 2007]. The recent evidence that $X^{Utx-}X^{Utx-}$ homozygous mice demonstrated a more severe phenotype than $X^{Utx-}Y^{Uty+}$ mice indicates that UTY can compensate for the loss of UTX in embryonic development [Shpargel et al., 2012]. Because mouse and human UTY show 75% identity, and 95% identity in the Jumonji C domain [Shpargel et al., 2012], it is likely that normal human males who have only one copy of *KDM6A* are supplemented by *UTY* in a demethylase-independent manner.

Interestingly, $X^{Utx-}Y^{Uty+}$ mice showed small body size [Shpargel et al., 2012]. Similarly, the human *KDM6A*-mutated group exhibited short stature and postnatal growth retardation.

Regarding our mutation detection methods, HRM analysis and Sanger sequencing are both imperfect. Next-generation sequencing is more sensitive (especially for single nucleotide variants and small insertions/deletions), faster, and cheaper due to multiple gene screening and the potential to multiplex. However, a microdeletion involving *MLL2* or *KDM6A* or low-level mosaicism of a single nucleotide variant might be missed by this method. Therefore, in patients who test mutation-negative, more comprehensive approaches might be necessary. In conclusion, we investigated *MLL2* and *KDM6A* mutations and their clinical consequences in patients with KS. The majority of the clinical features were observed at a similar frequency among patients with either *MLL2* or *KDM6A*-mutations. The genetic basis of the patients who tested mutation-negative (20–45%) remains elusive. Further studies are necessary to understand the whole picture of the genetic aspects of KS and its genotype–phenotype relationships.

ACKNOWLEDGMENTS

We thank the patients and their parents for participating in this work. We also thank Ms. Y. Yamashita, Ms. E. Koike, Ms. S. Sugimoto, Ms. N. Watanabe, Ms. K. Takabe, and Mr. T. Miyama for their technical assistance. This work was supported by research grants from the Ministry of Health, Labour and Welfare of Japan (H. Saitsu, N. Matsumoto, N. Miyake), the Japan Science and Technology Agency (N. Matsumoto), the Strategic Research Program for Brain Sciences (N. Matsumoto), a Grant-in-Aid for Scientific Research on Innovative Areas-(Transcription cycle)-from the Ministry of Education, Culture, Sports, Science and Technology of Japan (N. Matsumoto), a Grant-in-Aid for Scientific Research from the Japan Society for the Promotion of Science (N. Matsumoto), a Grant-in-Aid for Young Scientists from the Japan Society for the Promotion of Science (H.S., N. Miyake), the Takeda Science Foundation (N. Matsumoto, N. Miyake), the Yokohama Foundation for the Advancement of Medical Science (N. Miyake), and the Hayashi Memorial Foundation for Female Natural Scientists (N. Miyake).

REFERENCES

Adzhubei IA, Schmidt S, Peshkin L, Ramensky VE, Gerasimova A, Bork P, Kondrashov AS, Sunyaev SR. 2010. A method and server for predicting damaging missense mutations. Nat Methods 7:248–249.

Allen RC, Zoghbi HY, Moseley AB, Rosenblatt HM, Belmont JW. 1992. Methylation of *Hpa*II and *Hha*I sites near the polymorphic CAG repeat in the human androgen-receptor gene correlates with X chromosome inactivation. Am J Hum Genet 51:1229–1239.

Banka S, Howard E, Bunstone S, Chandler K, Kerr B, Lachlan K, McKee S, Mehta S, Tavares A, Tolmie J, Donnai D. 2012a. MLL2 mosaic mutations and intragenic deletion-duplications in patients with Kabuki syndrome. Clin Genet 83:467–471.

Banka S, Veeramachaneni R, Reardon W, Howard E, Bunstone S, Ragge N, Parker MJ, Crow YJ, Kerr B, Kingston H, Metcalfe K, Chandler K, Magee A, Stewart F, McConnell VP, Donnelly DE, Berland S, Houge G, Morton JE, Oley C, Revencu N, Park SM, Davies SJ, Fry AE, Lynch SA, Gill H, Schweiger S, Lam WW, Tolmie J, Mohammed SN, Hobson E, Smith A, Blyth M, Bennett C, Vasudevan PC, Garcia-Minaur S, Henderson A, Goodship J, Wright MJ, Fisher R, Gibbons R, Price SM, CdS D, Temple IK, Collins AL, Lachlan K, Elmslie F, McEntagart M, Castle B, Clayton-Smith J, Black GC, Donnai D. 2012b. How genetically heterogeneous is Kabuki syndrome?: MLL2 testing in 116 patients, review and analyses of mutation and phenotypic spectrum. Eur J Hum Genet 20:381–388.

Bogershausen N, Wollnik B. 2013. Unmasking Kabuki syndrome. Clin Genet 83:201–211.

Dubuc AM, Remke M, Korshunov A, Northcott PA, Zhan SH, Mendez-Lago M, Kool M, Jones DT, Unterberger A, Morrissy AS, Shih D, Peacock J, Ramaswamy V, Rolider A, Wang X, Witt H, Hielscher T, Hawkins C, Vibhakar R, Croul S, Rutka JT, Weiss WA, Jones SJ, Eberhart CG, Marra MA, Pfister SM, Taylor MD. 2013. Aberrant patterns of H3K4 and H3K27 histone lysine methylation occur across subgroups in medulloblastoma. Acta Neuropathol 125:373–384.

Greenfield A, Carrel L, Pennisi D, Philippe C, Quaderi N, Siggers P, Steiner K, Tam PP, Monaco AP, Willard HF, Koopman P. 1998. The UTX gene escapes X inactivation in mice and humans. Hum Mol Genet 7:737–742.

Hannibal MC, Buckingham KJ, Ng SB, Ming JE, Beck AE, McMillin MJ, Gildersleeve HI, Bigham AW, Tabor HK, Mefford HC, Cook J, Yoshiura K, Matsumoto T, Matsumoto N, Miyake N, Tonoki H, Naritomi K,

Kaname T, Nagai T, Ohashi H, Kurosawa K, Hou JW, Ohta T, Liang D, Sudo A, Morris CA, Banka S, Black GC, Clayton-Smith J, Nickerson DA, Zackai EH, Shaikh TH, Donnai D, Niikawa N, Shendure J, Bamshad MJ. 2011. Spectrum of MLL2 (ALR) mutations in 110 cases of Kabuki syndrome. Am J Med Genet Part A 155A:1511–1516.

Hong S, Cho YW, Yu LR, Yu H, Veenstra TD, Ge K. 2007. Identification of JmjC domain-containing UTX and JMJD3 as histone H3 lysine 27 demethylases. Proc Natl Acad Sci USA 104:18439–18444.

Ito N, Ihara K, Tsutsumi Y, Miyake N, Matsumoto N, Hara T. 2013. Hypothalamic pituitary complications in Kabuki syndrome. Pituitary 16:133–138.

Kokitsu-Nakata NM, Petrin AL, Heard JP, Vendramini-Pittoli S, Henkle LE, dos Santos DV, Murray JC, Richieri-Costa A. 2012. Analysis of MLL2 gene in the first Brazilian family with Kabuki syndrome. Am J Med Genet Part A 158A:2003–2008.

Kuroki Y, Suzuki Y, Chyo H, Hata A, Matsui I. 1981. A new malformation syndrome of long palpebral fissures, large ears, depressed nasal tip, and skeletal anomalies associated with postnatal dwarfism and mental retardation. J Pediatr 99:570–573.

Lan F, Bayliss PE, Rinn JL, Whetstine JR, Wang JK, Chen S, Iwase S, Alpatov R, Issaeva I, Canaani E, Roberts TM, Chang HY, Shi Y. 2007. A histone H3 lysine 27 demethylase regulates animal posterior development. Nature 449:689–694.

Lederer D, Grisart B, Digilio MC, Benoit V, Crespin M, Ghariani SC, Maystadt I, Dallapiccola B, Verellen-Dumoulin C. 2012. Deletion of KDM6A, a histone demethylase interacting with MLL2, in three patients with Kabuki syndrome. Am J Hum Genet 90:119–124.

Lee MG, Villa R, Trojer P, Norman J, Yan KP, Reinberg D, Di Croce L, Shiekhattar R. 2007. Demethylation of H3K27 regulates polycomb recruitment and H2A ubiquitination. Science 318:447–450.

Li Y, Bogershausen N, Alanay Y, Simsek Kiper PO, Plume N, Keupp K, Pohl E, Pawlik B, Rachwalski M, Milz E, Thoenes M, Albrecht B, Prott EC, Lehmkuhler M, Demuth S, Utine GE, Boduroglu K, Frankenbusch K, Borck G, Gillessen-Kaesbach G, Yigit G, Wieczorek D, Wollnik B. 2011. A mutation screen in patients with Kabuki syndrome. Hum Genet 130:715–724.

Makrythanasis P, van Bon BW, Steehouwer M, Rodriguez-Santiago B, Simpson M, Dias P, Anderlid BM, Arts P, Bhat M, Augello B, Biamino E, Bongers EM, Del Campo M, Cordeiro I, Cueto-Gonzalez AM, Cusco I, Deshpande C, Frysira E, Louise I, Flores R, Galan E, Gener B, Gilissen C, Granneman SM, Hoyer J, Yntema HG, Kets CM, Koolen DA, Marcelis CL, Medeira A, Micale L, Mohammed S, de Munnik SA, Nordgren A, Reardon SP, Revencu N, Roscioli T, Ruiterkamp-Versteeg M, Santos HG, Schoumans J, Schuurs-Hoeijmakers JH, Silengo MC, Toledo L, Vendrell T, van der Burgt I, van Lier B, Zweier C, Reymond A, Trembath RC, Perez-Jurado L, Dupont J, de Vries BB, Brunner HG, Veltman JA, Merla G, Antonarakis SE, Hoischen A. 2013. MLL2 mutation detection in 86 patients with Kabuki syndrome: A genotype–phenotype study. Clin Genet (In Press).

Micale L, Augello B, Fusco C, Selicorni A, Loviglio MN, Silengo MC, Reymond A, Gumiero B, Zucchetti F, D'Addetta EV, Belligni E, Calcagni A, Digilio MC, Dallapiccola B, Faravelli F, Forzano F, Accadia M, Bonfante A, Clementi M, Daolio C, Douzgou S, Ferrari P, Fischetto R, Garavelli L, Lapi E, Mattina T, Melis D, Patricelli MG, Priolo M, Prontera P, Renieri A, Mencarelli MA, Scarano G, della Monica M, Toschi B, Turolla L, Vancini L, Zatterale A, Gabrielli O, Zelante L, Merla G. 2011. Mutation spectrum of MLL2 in a cohort of Kabuki syndrome patients. Orphanet J Rare Dis 6:38.

Miyake N, Mizuno S, Okamoto N, Ohashi H, Shiina M, Ogata K, Tsurusaki Y, Nakashima M, Saitsu H, Niikawa N, Matsumoto N. 2013. KDM6A point mutations cause Kabuki syndrome. Hum Mutat 34:108–110.

Ng SB, Bigham AW, Buckingham KJ, Hannibal MC, McMillin MJ, Gildersleeve HI, Beck AE, Tabor HK, Cooper GM, Mefford HC, Lee C, Turner EH, Smith JD, Rieder MJ, Yoshiura K, Matsumoto N, Ohta T, Niikawa N, Nickerson DA, Bamshad MJ, Shendure J. 2010. Exome sequencing identifies MLL2 mutations as a cause of Kabuki syndrome. Nat Genet 42:790–793.

Niikawa N, Matsuura N, Fukushima Y, Ohsawa T, Kajii T. 1981. Kabuki make-up syndrome: A syndrome of mental retardation, unusual facies, large and protruding ears, and postnatal growth deficiency. J Pediatr 99:565–569.

Niikawa N, Kuroki Y, Kajii T, Matsuura N, Ishikiriyama S, Tonoki H, Ishikawa N, Yamada Y, Fujita M, Umemoto H, Iwama Y, Kondoh I, Fukushima Y, Nako Y, Matsui I, Urakami T, Aritaki S, Hara M, Suzuki Y, Chyo H, Sugio Y, Hasegawa T, Yamanaka T, Tsukino R, Yoshida A, Nomoto N, Kawahito S, Aihara R, Toyota S, Ieshima A, Funaki H, Ishitobi K, Ogura S, Furumae T, Yoshino M, Tsuji Y, Kondoh T, Matsumoto T, Abe K, Harada N, Miike T, Ohdo S, Naritomi K, Abushwereb AK, Braun OH, Schmid E. 1988. Kabuki make-up (Niikawa–Kuroki) syndrome: A study of 62 patients. Am J Med Genet 31:565–589.

Paulussen AD, Stegmann AP, Blok MJ, Tserpelis D, Posma-Velter C, Detisch Y, Smeets EE, Wagemans A, Schrander JJ, van den Boogaard MJ, van der Smagt J, van Haeringen A, Stolte-Dijkstra I, Kerstjens-Frederikse WS, Mancini GM, Wessels MW, Hennekam RC, Vreeburg M, Geraedts J, de Ravel T, Fryns JP, Smeets HJ, Devriendt K, Schrander-Stumpel CT. 2011. MLL2 mutation spectrum in 45 patients with Kabuki syndrome. Hum Mutat 32:E2018–E2025.

Prasad R, Zhadanov AB, Sedkov Y, Bullrich F, Druck T, Rallapalli R, Yano T, Alder H, Croce CM, Huebner K, Mazo A, Canaani E. 1997. Structure and expression pattern of human ALR, a novel gene with strong homology to ALL-1 involved in acute leukemia and to Drosophila trithorax. Oncogene 15:549–560.

Schuettengruber B, Chourrout D, Vervoort M, Leblanc B, Cavalli G. 2007. Genome regulation by polycomb and trithorax proteins. Cell 128:735–745.

Schwarz JM, Rodelsperger C, Schuelke M, Seelow D. 2010. MutationTaster evaluates disease-causing potential of sequence alterations. Nat Methods 7:575–576.

Shpargel KB, Sengoku T, Yokoyama S, Magnuson T. 2012. UTX and UTY demonstrate histone demethylase-independent function in mouse embryonic development. PLoS Genet 8:e1002964.

Tanaka R, Takenouchi T, Uchida K, Sato T, Fukushima H, Yoshihashi H, Takahashi T, Tsubota K, Kosaki K. 2012. Congenital corneal staphyloma as a complication of Kabuki syndrome. Am J Med Genet Part A 158A:2000–2002.

Tekin M, Fitoz S, Arici S, Cetinkaya E, Incesulu A. 2006. Niikawa–Kuroki (Kabuki) syndrome with congenital sensorineural deafness: Evidence for a wide spectrum of inner ear abnormalities. Int J Pediatr Otorhinolaryngol 70:885–889.

Torii Y, Yagasaki H, Tanaka H, Mizuno S, Nishio N, Muramatsu H, Hama A, Takahashi Y, Kojima S. 2009. Successful treatment with rituximab of refractory idiopathic thrombocytopenic purpura in a patient with Kabuki syndrome. Int J Hematol 90:174–176.

Tsurusaki Y, Kobayashi Y, Hisano M, Ito S, Doi H, Nakashima M, Saitsu H, Matsumoto N, Miyake N. 2013. The diagnostic utility of exome sequencing in Joubert syndrome and related disorders. J Hum Genet 58:113–115.

Xu J, Deng X, Watkins R, Disteche CM. 2008. Sex-specific differences in expression of histone demethylases Utx and Uty in mouse brain and neurons. J Neurosci 28:4521–4527.

Research article

PRKDC mutations in a SCID patient with profound neurological abnormalities

Lisa Woodbine,[1] Jessica A. Neal,[2] Nanda-Kumar Sasi,[2] Mayuko Shimada,[3] Karen Deem,[4] Helen Coleman,[5] William B. Dobyns,[6] Tomoo Ogi,[3,7] Katheryn Meek,[2] E. Graham Davies,[8] and Penny A. Jeggo[1]

[1]Genome Damage and Stability Centre, University of Sussex, Brighton, United Kingdom. [2]College of Veterinary Medicine, Department of Microbiology and Molecular Genetics, and Department of Pathobiology and Diagnostic Investigation, Michigan State University, East Lansing, Michigan, USA. [3]Nagasaki University Research Centre for Genomic Instability and Carcinogenesis (NRGIC), Nagasaki, Japan. [4]Department of Paediatrics, Queen Alexandra Hospital, Portsmouth, United Kingdom. [5]Solent NHS Trust, Portsmouth, United Kingdom. [6]Center for Integrative Brain Research, Seattle Children's Hospital, Seattle, Washington, USA. [7]Department of Molecular Medicine, Atomic Bomb Disease Institute, Graduate School of Biomedical Sciences, Nagasaki, Japan. [8]Centre for Immunodeficiency, Great Ormond Street Hospital and Institute of Child Health, London, United Kingdom.

The DNA-dependent protein kinase catalytic subunit (DNA-PKcs; encoded by *PRKDC*) functions in DNA non-homologous end-joining (NHEJ), the major DNA double strand break (DSB) rejoining pathway. NHEJ also functions during lymphocyte development, joining V(D)J recombination intermediates during antigen receptor gene assembly. Here, we describe a patient with compound heterozygous mutations in *PRKDC*, low DNA-PKcs expression, barely detectable DNA-PK kinase activity, and impaired DSB repair. In a heterologous expression system, we found that one of the *PRKDC* mutations inactivated DNA-PKcs, while the other resulted in dramatically diminished but detectable residual function. The patient suffered SCID with reduced or absent T and B cells, as predicted from *PRKDC*-deficient animal models. Unexpectedly, the patient was also dysmorphic; showed severe growth failure, microcephaly, and seizures; and had profound, globally impaired neurological function. MRI scans revealed microcephaly-associated cortical and hippocampal dysplasia and progressive atrophy over 2 years of life. These neurological features were markedly more severe than those observed in patients with deficiencies in other NHEJ proteins. Although loss of DNA-PKcs in mice, dogs, and horses was previously shown not to impair neuronal development, our findings demonstrate a stringent requirement for DNA-PKcs during human neuronal development and suggest that high DNA-PK protein expression is required to sustain efficient pre- and postnatal neurogenesis.

Introduction

DNA nonhomologous end-joining (NHEJ) represents the major DNA double strand break (DSB) repair process in mammalian cells (1, 2). Thus, cells, mice, and patients defective in NHEJ proteins show markedly reduced DSB repair and radiosensitivity. NHEJ also functions during immune development due to its requisite role in V(D)J recombination (3). V(D)J recombination mediates immunoglobulin and T cell receptor gene assembly from variable (V), diversity (D), and joining (J) gene segments. Recombination is initiated by the RAG1/2 endonuclease, which introduces DSBs at recombination signal sequences (RSSs). The DNA ends, including the sequences encoding the antigen receptors (termed *coding ends*), have hairpinned termini; the RSSs are blunt ended. Rejoining of these recombination intermediates requires NHEJ proteins. Consequently, NHEJ defects in animals and humans causes SCID with reduced or absent T and B cells.

6 core NHEJ components assemble as 2 complexes (1). The Ku70/80 heterodimer is the DNA double-stranded (ds) end recognition protein, binding DNA ds ends with high affinity. Ku recruits the DNA-dependent protein kinase catalytic subunit (DNA-PKcs; encoded by *PRKDC*), generating the DNA-PK holoenzyme. The DNA-PK complex prevents unbridled exonuclease digestion of DNA ends, enhances appropriate end-processing, and recruits the ligation complex, which encompasses XRCC4, DNA ligase IV, and XLF (also known as cernunnos). Ionizing radiation–induced (IR-induced) DSBs are rejoined with 2 component kinetics: a fast process rejoins approximately 85% of DSBs, whereas the remaining 15% are rejoined with slower kinetics (4). Core NHEJ proteins (Ku, DNA-PKcs, DNA ligase IV, XRCC4, and XLF) are required for both processes in G0/G1 phase. However, the nuclease, Artemis, functions uniquely in the slow process. Artemis is also required to cleave hairpin coding ends during V(D)J recombination (5). DNA ligase IV and XRCC4 are essential for NHEJ, whereas XLF enhances the process, but is not essential. Similarly, DNA-PKcs is facilitating, but not essential, for the fast process (6, 7). However, there is a more stringent requirement for DNA-PKcs for the slow DSB repair process, similar to the need for Artemis (8). Although DNA-PKcs has Artemis-independent functions, an important role of DNA-PKcs lies in activating Artemis (5, 9).

The NHEJ genes have been inactivated in mice with differing consequences. Ku-defective mice are viable but have SCID, severe growth retardation, and premature aging (10). Mice lacking XRCC4 or DNA ligase IV are embryonic lethal due to increased neuronal apoptosis (11, 12). Mice lacking XLF are, in contrast, viable with mild immunodeficiency and have no marked neuronal phenotype (13). Finally, mice lacking DNA-PKcs are viable, with no overt phenotype other than SCID (14). Spontaneous mutations in *PRKDC* have also been described in inbred horses and dogs (15–17). Such animals have SCID, but otherwise develop normally, although DNA-PKcs deficiency in dogs causes a mild

Conflict of interest: The authors have declared that no conflict of interest exists.
Citation for this article: *J Clin Invest.* 2013;123(7):2969–2980. doi:10.1172/JCI67349.

intrauterine growth delay and cellular proliferation deficits (17). Importantly, neurological development is normal. The mutational changes in these animal models confer null phenotypes in all assays used, which suggests either that DNA-PKcs is nonessential or that less than 1% activity suffices for viability and development in these animal models.

Approximately 30% of SCID patients have V(D)J recombination defects, with approximately 70% having mutations in *RAG1* or *RAG2* (18, 19). Less commonly, SCID can be caused by mutations in NHEJ genes. Importantly, LIGIV syndrome and XLF patients harbor hypomorphic mutations in the genes encoding DNA ligase IV or XLF, respectively, and display T and B cell lymphocytopenia, growth delay, and microcephaly (20, 21). Generally, these patients do not have profound neurodevelopmental problems, and the neuronal deficit is not progressive postnatally. A mouse model for LIGIV syndrome shows small growth and elevated apoptosis in the embryonic neuronal stem and progenitor cell compartment (22). One LIGIV patient who received radiotherapy died of radiation morbidity (23). Collectively, these findings suggest that reduced DNA ligase IV activity confers clinical radiosensitivity and additionally that NHEJ functions during embryonic neuronal development. In contrast, mutations in the gene encoding Artemis are often null and confer radiosensitive SCID (RS-SCID), but no overt reduced growth or microcephaly (24). A single patient with a homozygous missense mutation in *PRKDC* has been previously reported (25). The mutational change did not affect DNA-PKcs expression nor enzymatic activity, but impaired Artemis activation. Like Artemis-defective patients, this DNA-PKcs–deficient patient had SCID but was otherwise developmentally normal.

Given the occurrence of spontaneous mutations in *PRKDC* in dogs and horses, it is surprising that patients with mutations in *PRKDC* have not been more frequently reported. However, recent work has strongly suggested that the DNA-PK complex is essential in humans. Elegant work from Hendrickson and colleagues has demonstrated that homozygous loss of Ku in human cells causes loss of viability due to rapid telomere shortening (26–28). In contrast, disruption of *PRKDC* in the same genetic background had a more modest impact on telomere maintenance and did not preclude viability, although it did confer profound proliferation and genomic stability defects (29). It has therefore been suggested that a *PRKDC* null mutation would be incompatible with life in humans (16, 25, 30).

Here, we identified a SCID patient with substantially reduced DNA-PKcs protein levels, undetectable DNA-PK activity, and impaired DSB rejoining attributable to loss of DNA-PK activity. The patient had a point mutational change in 1 allele that severely impaired but did not abrogate DNA-PK activity, strongly suggesting that it represents a hymophric mutation. A cDNA product resulting from aberrant splicing was also detected. The patient's cells had substantially reduced DNA-PKcs protein levels and impaired DSB rejoining that was attributable to loss of DNA-PK activity. The mutational change in 1 allele resulted in the loss of an exon and appeared to be inactivating; the other mutational change, however, was hypomorphic. The patient had marked neurological abnormalities, remarkably more severe than observed in hitherto described NHEJ-defective SCID patients. Strikingly, neuronal atrophy was observed postnatally. Our findings highlight an important role for DNA-PKcs during neuronal development and maintenance in humans.

Results

Clinical features. Male patient NM720, the first child of nonconsanguineous parents, exhibited poor intrauterine growth on antenatal ultrasounds. There was prolonged rupture of the membranes and an abnormal cardiotocograph, leading to delivery by caesarean section at 37 weeks. Birth weight was 2.1 kg (0.4th–2nd percentile), and occipitofrontal circumference (OFC) was 32.2 cm (9th–25th percentile). He was admitted to the hospital at 3 weeks of age with suspected sepsis and persistent oral and perineal candidiasis. A diagnosis of SCID was made at 5 weeks with complete absence of T and B cells, normal NK cell numbers, and undetectable IgA and IgM levels ($T^-B^-NK^+$). At 2 years of age, there were still no detectable circulating T cells (0.02×10^9 cells/l) and no B cells. The patient was noted to be microcephalic (OFC, 31.5 cm; <0.4th percentile) and dysmorphic with prominent forehead, wide nasal bridge, deep-set eyes, long philtrum with thin upper lip, small chin, low-set ears with overfolded helices, overlapping fingers, and postaxial polysyndactyly of the right foot. He had micropenis, but with normal descended testes and normal pituitary function. At gastrostomy insertion, the stomach was noted to be very small and nondistensible. A spleen was detectable by ultrasound. Neurologically, the patient showed little developmental progress with very poor head growth (OFC, 35.2, 36.8, 38.6, and 39.2 cm at 4, 6.5, 11, and 30 months, respectively). He developed seizures. Investigations including cerebrospinal fluid examination failed to reveal any microbial pathogens. He had bilateral profound sensorineural hearing loss on brain stem–evoked responses and severe visual impairment, with electroretinograms showing markedly degraded responses and occipital flash and binocular occipital pattern visual evoked potentials showing degraded, delayed, broadened, and inconsistent responses. At 29 months of age, his neurodevelopmental level was that of a 3- to 4-month-old. He died at 31 months of age with intractable seizures.

Neurological imaging of the patient at 3 months and 2 years of age. An MRI scan undertaken at 3 months of age revealed microcephaly and an atypical cortical malformation consisting of a diffusely reduced number and depth of sulci (i.e., simplified gyral pattern), mild frontal pachygyria with the frontal cortex relatively thicker than the posterior cortex (4 mm versus 2–3 mm), and a blurred cortical–white matter border (Figure 1). The hippocampi were small and dysplastic, and the posterior pituitary bright spot was absent, suggestive of disruption of the posterior pituitary-hypothalamic axis. Additional changes included hypomyelinated white matter, mildly enlarged lateral ventricles, thin and mildly short corpus callosum, cavum septi pellucidi and cavum vergae, and moderate cerebellar vermis hypoplasia. In summary, the brain images demonstrated microcephaly-associated cortical and hippocampal dysplasia that differed from lissencephaly. The irregular or pebbled surface and microgyri that characterize typical or "coarse" polymicrogyria were not seen, although the overall immature appearance might have obscured the more subtle or "delicate" form of polymicrogyria (31). A second MRI scan at 2.4 years showed striking progressive atrophy involving all brain regions compared with the first scan (Figure 1), corresponding to one of the major microcephaly groups (group 3; microcephaly with simplified gyri and enlarged extra-axial space) defined in a recent paper (32).

Defective DSB repair in patient fibroblasts. Patient fibroblasts were established to assess the possibility of a RS-SCID disorder. Poor cloning efficiency of the primary fibroblasts precluded clonogenic radiosensitivity analysis. An hTERT immortalized line, NM720

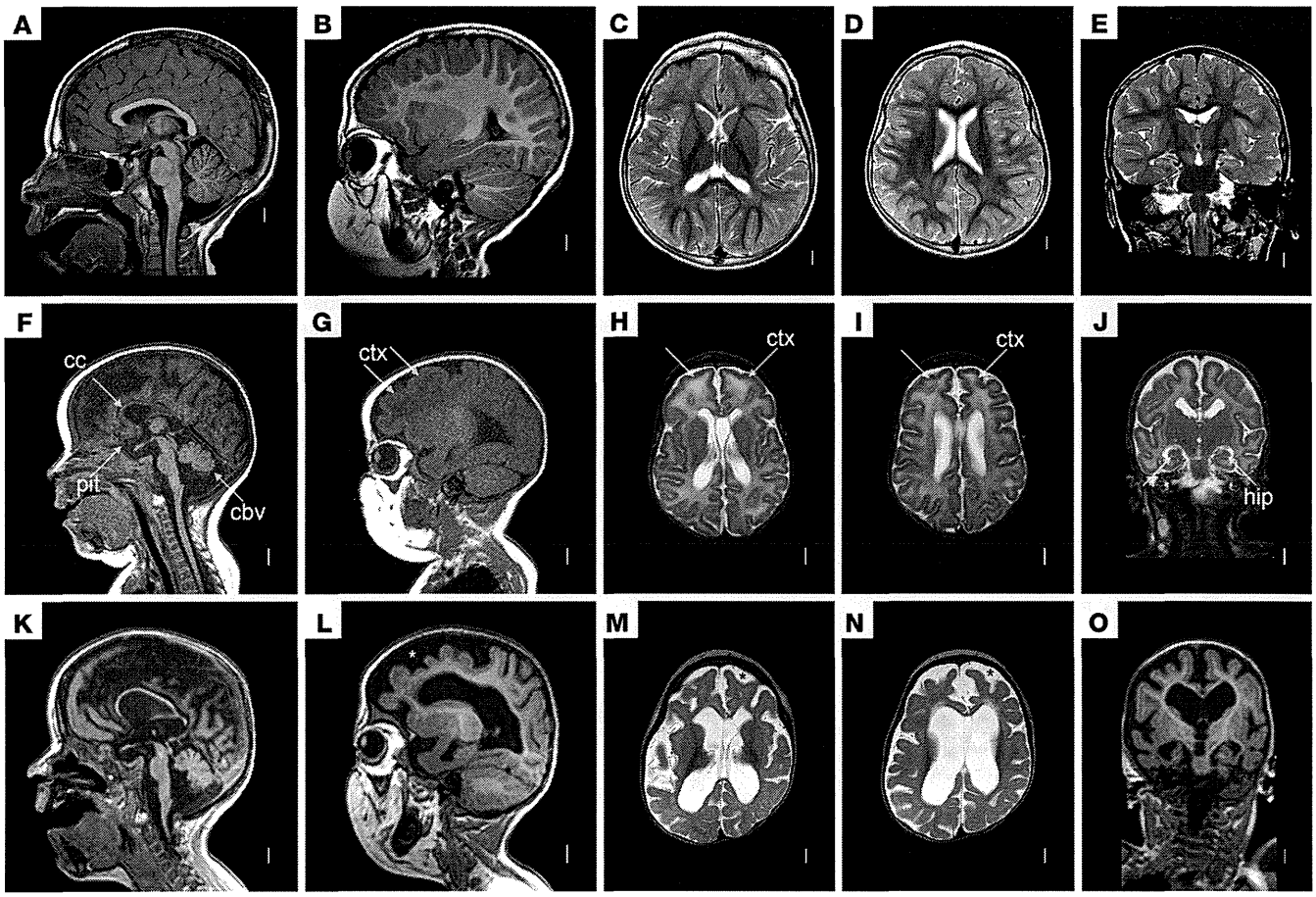

Figure 1
MRI scan images of patient NM720. Brain MRI in a normal 3-year-old child (**A**–**E**) and in patient NM720 at 3 months (**F**–**J**) and 2 years (**K**–**O**). In the patient, midline sagittal T1-weighted images (**F** and **K**) showed an absent pituitary bright spot (pit), thin and short corpus callosum (cc), and small uprotated cerebellar vermis (cbv). Parasagittal (**G** and **L**) and axial T2-weighted (**H**, **I**, **M**, and **N**) images showed reduced number of gyri, and mildly thick cortex with blurred gray-white border (ctx). Coronal images (**J** and **O**) showed the same changes in the cortex, as well as mildly small hippocampi. Striking progressive atrophy was seen involving all brain regions on the second scan (asterisks in **L**–**N**).

hTERT, was established, but these cells also plated poorly, precluding analysis. We have previously exploited γH2AX foci analysis to monitor DSB repair (8). This assay uses nondividing cells, avoiding complications from γH2AX formation during replication, and can be used with poorly growing cells. Enumeration of γH2AX formation and loss after 3 Gy IR revealed a pronounced DSB repair defect, which was distinct from that observed in either LIGIV syndrome or Artemis-defective patient cells (Figure 2A). LIGIV syndrome cells (lines 180BR and 495BR) displayed a pronounced DSB repair defect at 2 and 6 hours after IR. However, the mutational changes identified in patients are hypomorphic, and cells retain residual ligase activity, consistent with the findings in mice that DNA ligase IV is essential. Thus, DSB repair ensues slowly, as evidenced by the diminished levels of residual DSBs from 24 to 48 hours (see also ref. 33). Interestingly, the mutational changes in 495BR cells were more severe than those in 180BR cells, resulting in a greater DSB repair defect, which also correlates with more severe clinical features. A similar profile is observed for XLF-deficient cells (6). In contrast, the repair defect in an Artemis-null cell line, F02/385, was persistent but only evident at later times (beginning at 24 hours), since Artemis is dispensable for the fast DSB repair process but essential for the slow DSB repair component (8). In contrast to these phenotypes, patient cells displayed a small defect at 2 hours, but the defect was retained at 8 days after IR (Figure 2, A and B). 709BR cells, derived from the patient's mother, showed normal repair; cells from the father were not available. This profile closely corresponded to, but was milder than, that observed in *Prkdc*$^{-/-}$ mouse embryonic fibroblasts (data not shown) and in control human cells treated with the DNA-PK–inhibiting drug (DNA-PKi) NU7441 (Figure 2B). Furthermore, addition of DNA-PKi to patient cells was not additive to this repair defect and was indistinguishable from DNA-PKi–treated control cells. These findings are consistent with an epistatic relationship and raise the possibility that there could be a hypomorphic defect in DNA-PKcs in patient cells. Collectively, these findings suggest that the patient is defective in an NHEJ protein and implicate DNA-PKcs as a candidate defect.

Severely reduced DNA-PKcs expression and activity in patient cells. Next, we carried out immunoblotting of the 7 core NHEJ proteins as well as LIS1, a protein frequently deficient in patients displaying lissencephaly, which was also evaluated as a causal defect (Figure 3A). Strikingly, although most NHEJ proteins were expressed at

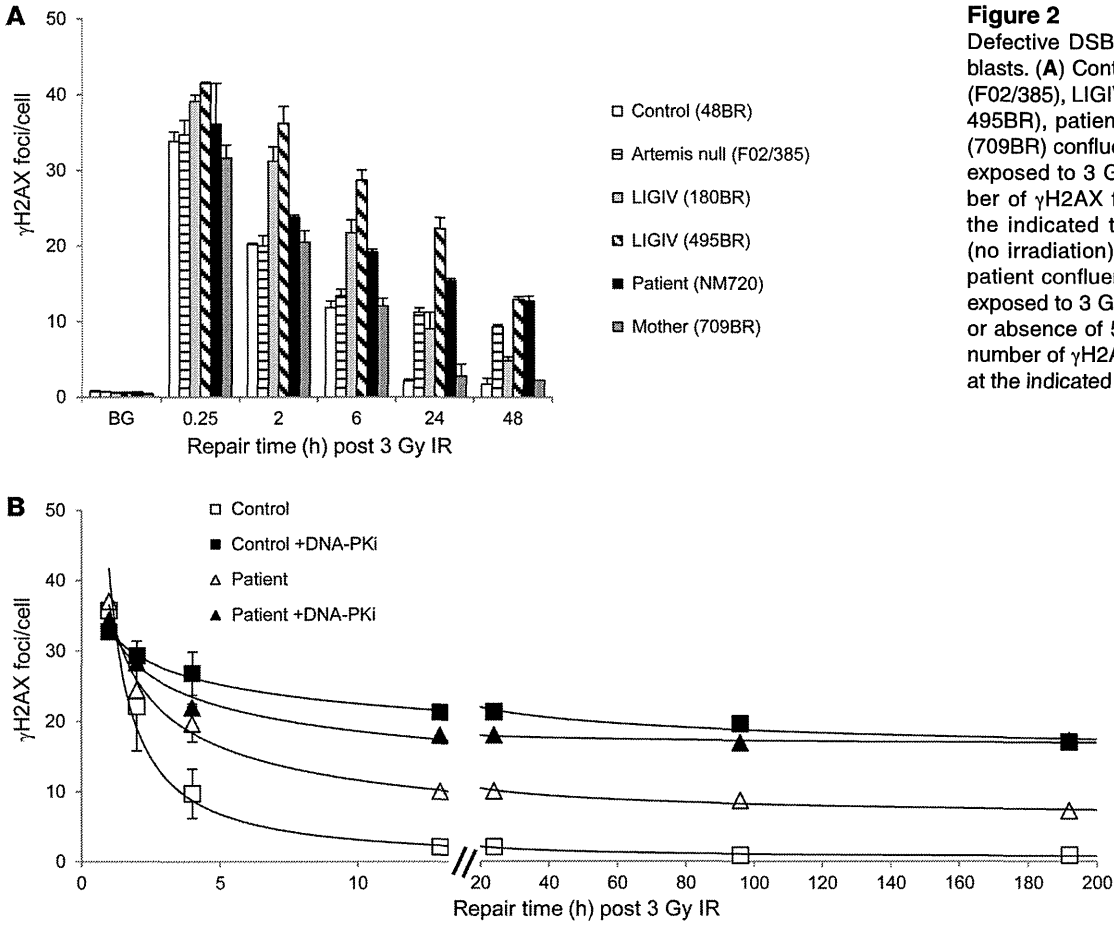

Figure 2
Defective DSB repair in patient fibroblasts. (**A**) Control (48BR), Artemis null (F02/385), LIGIV syndrome (180BR and 495BR), patient (NM720), and mother (709BR) confluent G0 phase cells were exposed to 3 Gy γ-rays, and the number of γH2AX foci was determined at the indicated times. BG, background (no irradiation). (**B**) 1BR3 control and patient confluent G0 phase cells were exposed to 3 Gy γ-rays in the presence or absence of 5 μM DNA-PKi, and the number of γH2AX foci was enumerated at the indicated times.

normal levels, DNA-PKcs expression was dramatically reduced in patient cells. However, residual DNA-PKcs protein was detectable and verified by comparison with M059J, a human tumor cell line that lacks DNA-PKcs expression (34). Furthermore, the patient's mother's cells showed approximately 50% of the level of DNA-PKcs observed in control cells (Figure 3B).

Additionally, quantitative analysis of DNA-PKcs activity present in hTERT fibroblasts derived from control (1BR3), patient, and mother cells revealed no detectable DNA-PK activity in patient hTERT cells and approximately 50% of the level of WT activity in the mother's hTERT cells (Figure 3C). This assay is extremely sensitive, and we estimate that 1% of the control level would be detectable. These findings confirmed a profound defect in DNA-PK activity in patient cells.

Mutational changes in PRKDC. DNA-PKcs is one of the largest known cDNAs (35). To search for mutational changes, 9 overlapping PCR fragments from DNA-PKcs cDNA were amplified and sequenced from control and patient, revealing a c.10721C>T mutational change in 1 allele of the patient creating an alanine to valine amino acid substitution at the highly conserved residue 3574 (p.A3574V) (Figure 4, A and E). The mother also carried this mutational change.

Additionally, we observed a double sequence commencing at c.1624, which represents the boundary between exons 15 and 16, suggesting that exon 16 might be deleted in the patient (Figure 4B). To substantiate this, primers were designed in exons 15 and 17. RT-PCR using cDNA derived from control cells revealed a single product, whereas 2 discrete bands were observed using patient cells (Figure 4C). The RT-PCR amplification products were cloned, and individual clones were sequenced. Whereas all clones from the control cell line showed the anticipated sequence encompassing exon 16, approximately 50% (10 of 20) of the clones derived from the patient lacked exon 16 (the other 50% included exon 16). Importantly, this deletion did not affect the reading frame. This is consistent with the finding that 50% of the RT-PCR amplification products were derived from the exon 16–deleted cDNA, demonstrating that there was no substantial nonsense-mediated decay (NMD). To confirm normal expression of the exon 16–deleted allele, we performed quantitative RT-PCR analyses to determine the transcript levels of the full-length WT, exon 16–deleted, and mutant *PRKDC* alleles in the patient, the mother, and a normal control (Figure 4D). The mutant c.10721C>T allele was expressed to similar extents in the patient and mother, while no mutant cDNA was detected in the normal control. Importantly, the WT c.10721C allele was expressed nearly 2-fold higher in the normal control relative to the patient or the mother. This strongly indicates that the exon 16–deleted, c.10721C, and c.10721C>T alleles are expressed at similar levels and thus are equally stable.

Finally, we examined DNA-PKcs cDNA from 15 normal individuals and did not observe any abnormal splicing involving exon 16, which suggests that this is not a common splice variant. Sequencing of exon 16 from the patient's genomic

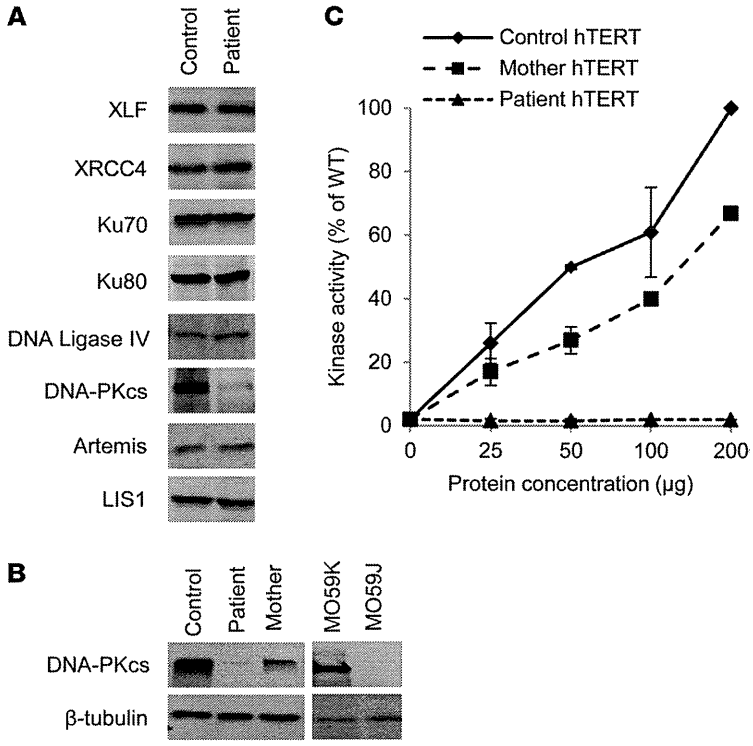

Figure 3

Reduced DNA-PKcs expression and activity in patient cells. (**A**) Western blotting analysis shows reduced DNA-PKcs protein in patient cells. Whole cell extracts (50 μg) from 1BR3 control or patient cells were processed for Western blotting using the indicated antibodies. (**B**) Western blotting analysis confirmed that residual DNA-PKcs protein was validated against human tumor cells, M059K and M059J. M059J cells are null for DNA-PKcs (53). (**C**) DNA-PK–dependent kinase activity was examined using whole cell lysates from 1BR3 control, mother, and patient immortalized primary hTERT fibroblasts.

DNA revealed a normal sequence. Additionally, intron 16 was sequenced from the patient, and an IVS16+1510insA mutation 700 bp upstream of the splice site was identified. This change was not present in the mother's genomic DNA (Supplemental Figure 1; available online with this article; doi:10.1172/JCI67349DS1). However, considering the substantial distance of this change from the exon 15/16 splice site, it is unclear whether this represents the causal mutational change causing exon skipping. This change, however, was not a reported polymorphism or SNP (Supplemental Figure 1).

In summary, patient cells harbored mutational changes in *PRKDC*. The maternally derived allele generated a p.A3574A mutant protein. Additionally, we identified a splicing abnormality generating a cDNA lacking exon 16. The location of these mutational changes and critical domains in *PRKDC* are shown in Figure 4E.

PRKDC complements the DSB repair defect observed in patient cells. To test complementation, a previously constructed GFP-tagged full-length DNA-PKcs cDNA was used (36). 1BR3 control and patient hTERT fibroblasts were transfected with DNA-PKcs cDNA and exposed to 3 Gy IR 48 hours later, and γH2AX foci were enumerated 0.25, 8, and 16 hours after IR in cells staining positively for GFP. GFP staining was used to identify and analyze only transfected cells, which represented less than 10% of the cell population (expected given the size of the DNA-PKcs cDNA and use of patient fibroblasts). Strikingly, we observed almost full correction of the DSB repair defect in patient hTERT cells expressing DNA-PKcs (Figure 5). As a control, the DNA-PKcs cDNA was also transfected into 180BR LIGIV syndrome TERT cells; as expected, no complementation of the DNA repair defect was observed. Similarly, transfection of 1BR3 control hTERT cells or the patient's mother's hTERT cells with DNA-PKcs cDNA did not affect the cells' rate of DSB repair. Collectively, these data provide compelling evidence that the DSB repair defect observed in patient cells is a consequence of impaired DNA-PKcs function.

p.A3574V or loss of exon 16 dramatically impairs DNA-PK function and activity. A3574, which lies outside the kinase domain within the large FAT domain, is a highly conserved residue in DNA-PKcs (Figure 4E). Nonetheless, an alanine to valine substitution does not represent a dramatic change. To gain further insight into whether p.A3574V affects DNA-PKcs function, this substitution was introduced into DNA-PKcs cDNA by site-directed mutagenesis and cloning. WT and mutant *PRKDC* constructs were introduced into V3, a CHO cell line that lacks functional DNA-PKcs (37). Stable clones were isolated, and those that expressed equivalent levels of DNA-PKcs (as determined by immunoblotting) were selected for further study. To examine whether the p.A3574V substitution affects DNA-PKcs function in response to damage-induced DSBs, clonogenic survival assays were performed after exposure to the DSB-inducing agent zeocin (Figure 6A). Whereas WT human DNA-PKcs substantially reversed the zeocin sensitivity of V3 cells, cells expressing the p.A3574V mutant were as sensitive to zeocin as those transfected with empty vector. We conclude that A3574V DNA-PKcs substantially disrupts DNA-PKcs function in response to damage-induced DSBs.

We next tested whether A3574V DNA-PKcs could function to repair RAG-induced DSBs during V(D)J recombination. V(D)J recombination can be assessed in somatic cells using plasmid substrates introduced into cultured cells together with the RAG recombination genes (38). V3 cells were transfected with RAG expression vectors, a recombination substrate that assesses coding end-joining, as well as WT, mutant, or no DNA-PKcs cDNA. As expected, WT DNA-PKcs supported substantial levels of coding end-joining (Figure 6B). Although A3574V DNA-PKcs cDNA supported considerably less coding end-joining than WT DNA-PKcs, a low but measurable level of coding joints were recovered, which suggests that A3574V DNA-PKcs retains some functional capacity. We considered that this low level of coding end-joining might be analogous to the "leaky" joining observed in mouse or hamster cells that lack DNA-PKcs, where the leaky joints are thought to be mediated by an alternative NHEJ pathway. Characteristics of leaky joining include excessive nt loss and long P elements. To examine the junctions formed from the rejoined joints, DNA was prepared from the rejoined plasmid substrates and sequenced. Surprisingly, coding joints mediated by A3574V DNA-PKcs were indistinguishable from those formed by WT DNA-PKcs (Table 1). We conclude that although A3574V DNA-PKcs cannot support normal levels of end-joining, end process-

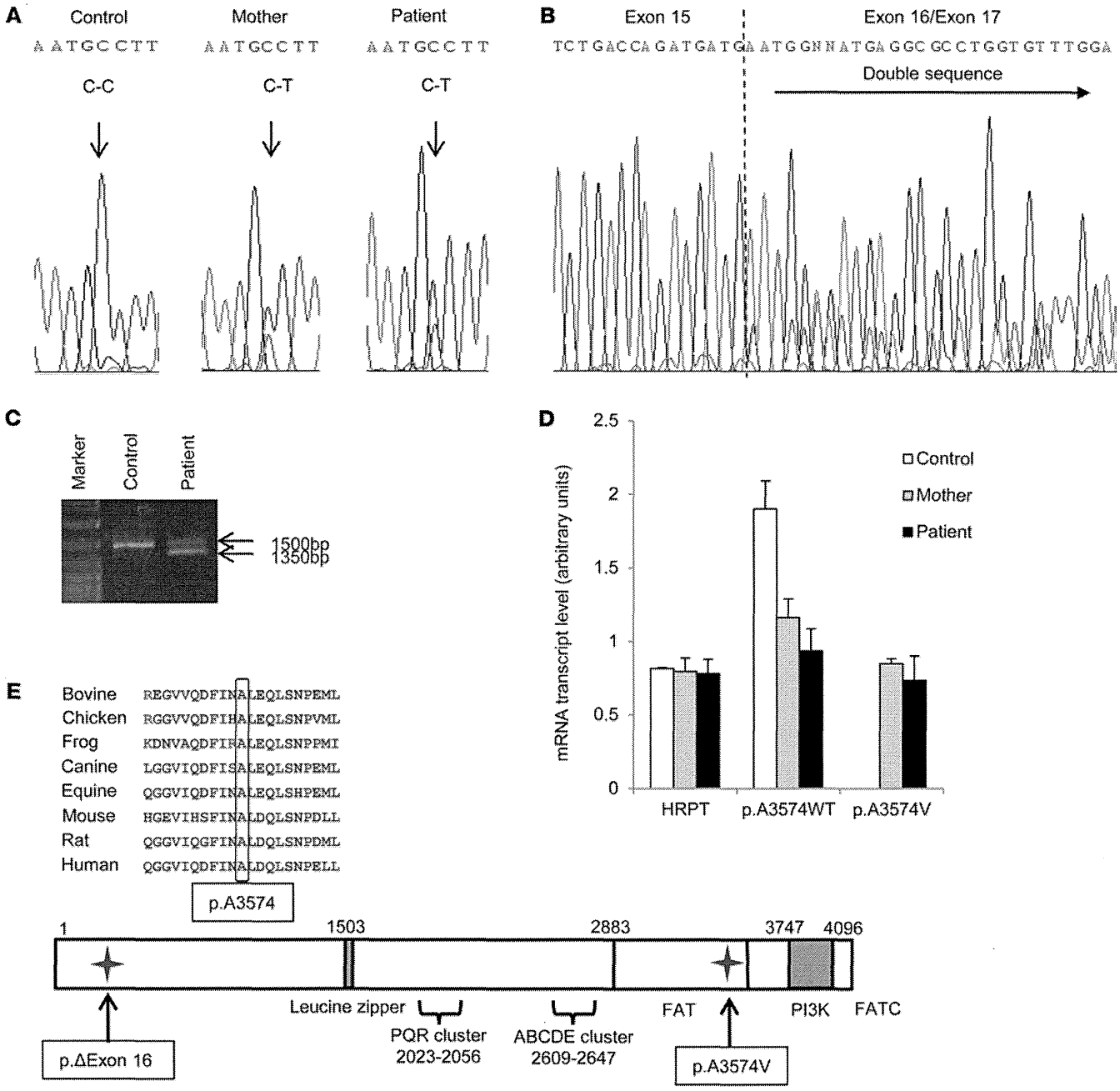

Figure 4

Identification of mutational changes in *PRKDC* cDNA. (**A**) Dye-terminator sequence figures illustrating the c.10721C>T mutational change in 1 allele of the patient and mother. (**B**) Dye-terminator sequence figures illustrating a double sequence commencing at c.1624, the bp at the boundary between exons 15 and 16. (**C**) RT-PCR amplification products using primers located in exons 15 and 17. Control cells yielded a single product of the size anticipated for the presence of exon 16. Patient cells yielded 2 bands, the smaller of which was the size expected for a product lacking exon 16. The greater signal could be the result of enhanced amplification of a smaller fragment. (**D**) mRNA transcript levels, determined using primers specific for HPRT, the WT p.A3574 allele (*PRKDC* c.10712C), or the mutant p.A3574V allele (*PRKDC* c.10712C>T). All cell lines showed equal expression of HPRT. cDNA of 48BR control cells had 2-fold greater levels of the WT allele compared with cDNA from mother or patient cells, which expressed the same level of the p.A3574 and p.A3574V mutant alleles. (**E**) Conservation of the A3574 residue between species and location of the identified mutational changes in *PRKDC* in relation to important domains.

ing of DNA ends is normal, consistent with the notion that the A3574V mutant supports reduced levels of classical NHEJ.

Finally, we examined whether A3574V DNA-PKcs retains enzymatic activity. DNA-PK from V3 extracts was pulled down onto DNA cellulose beads, and enzymatic activity was measured using a biotinylated p53 peptide as a substrate. Virtually no activity was detectable from cells expressing A3574V DNA-PKcs (Figure 6C). This was somewhat surprising, since kinase activity has previously

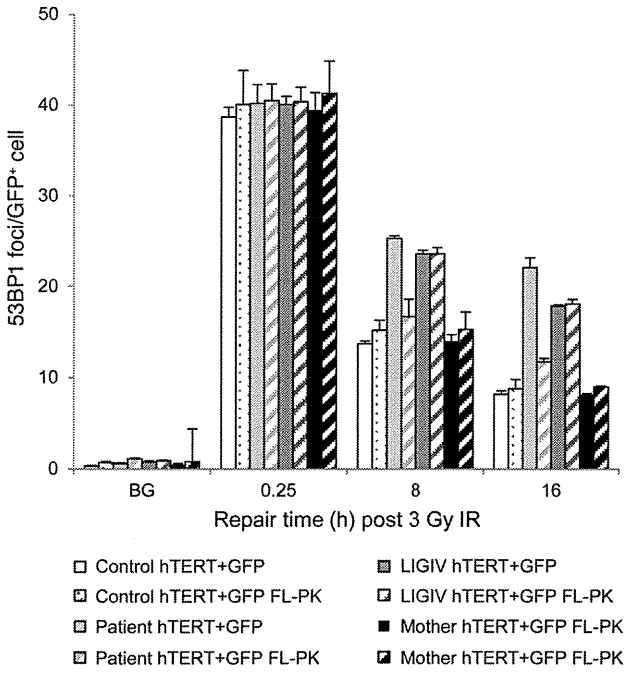

Figure 5
DNA-PKcs cDNA complements the DSB repair defect observed in patient cells. GFP-tagged full-length DNA-PKcs cDNA (GFP FL-PK) or GFP empty vector (GFP) was transfected into 1BR3 control, patient, 180BR LIGIV syndrome, and mother hTERT cells. 24 hours after transfection, cells were irradiated with 3 Gy γ-rays, and 53BP1 foci in GFP+ cells were enumerated at 8 and 16 hours. The identification of GFP+ cells was critical, since the transfection frequency using the large DNA-PKcs cDNA and human fibroblasts was low (<1%). Substantial correction of the DSB repair defect of patient cells was observed upon expression of full-length DNA-PKcs cDNA. No correction was observed after transfection of full-length DNA-PKcs cDNA into LIGIV syndrome cells.

been shown to be essential for the ability of DNA-PKcs to support coding end-joining. Thus, DNA-PKcs autophosphorylation was also assessed as an alternative measure of enzymatic activity, using a phosphospecific antibody to pS2056 DNA-PKcs, a well-studied DNA-PKcs autophosphorylation site (39). Immunoblotting of in vitro kinase reaction proteins (after 5 or 30 minutes) revealed that A3574V DNA-PKcs underwent autophosphorylation, albeit with slower kinetics and with less efficiency than the WT protein (Figure 6D). We conclude that A3574V DNA-PKcs has residual but substantially impaired catalytic activity.

Loss of exon 16 did not cause a frameshift, but the encoded protein lacked amino acids 541–592. Our previous studies have shown that *PRKDC* does not tolerate deletions (40, 41). Furthermore, the deleted region is highly conserved in vertebrate *PRKDC* and, from the available structural studies, is predicted to reside within the N-terminal "pincer" domain. DNA-PKcs cDNA lacking exon 16 was generated, and its function was assessed in V3 cells. DNA-PKcs expression in V3 clones expressing the exon 16 deletion was considerably lower than in cells expressing WT protein (Figure 6). Moreover, the clones did not reverse the zeocin-sensitive phenotype of V3 cells, failed to support VDJ coding end resolution, and yielded no detectable DNA-PKcs activity using the assays described above. Collectively, these findings provide strong evidence that loss of exon 16 dramatically affects function and likely represents a null mutational change. This finding is consistent with our previous DNA-PKcs mutational studies showing that small N-terminal deletions completely ablate function and that other exon-skipped DNA-PKcs variants are similarly nonfunctional (40, 41).

In summary, although cells expressing A3574V DNA-PKcs were similarly sensitive to zeocin-induced DSBs as cells expressing no DNA-PKcs, the mutant protein did retain residual catalytic activity, supporting a low level of coding end-joining. This is consistent with previous suggestions that very low levels of DNA-PKcs activity are sufficient to support V(D)J recombination but insufficient to reverse the radiosensitive phenotype caused by DNA-PKcs deficiency (30, 42). Finally, since neither the A3574V DNA-PKcs nor the exon 16 deletion increased zeocin sensitivity in cells completely lacking DNA-PKcs, we conclude that the phenotype cannot be attributed to a dominant negative effect on NHEJ but results from loss of DNA-PK activity. The lack of a dominant negative impact is further substantiated by the complementation of DSB repair in patient cells by GFP-tagged DNA-PKcs.

Discussion

Here, we identified an immunodeficient patient with impaired DSB repair, affecting mutations in *PRKDC*, and dramatically reduced DNA-PK activity. Although a previous patient with mutations in *PRKDC* has been reported, the homozygous mutational change exerted a subtle impact that specifically affected Artemis activation and conferred no overt clinical features other than combined immunodeficiency (25). Thus, our findings represent the first description of a patient with substantially reduced DNA-PK activity that impairs core NHEJ. The patient displayed a marked neurological phenotype substantially more severe than that of previously described LIGIV syndrome or XLF-deficient patients, who normally show mild microcephaly (20, 21). The cortical disorganization bears some resemblance to the malformation described in a fetus carrying a balanced translocation that disrupted the gene encoding XLF (43). The fetus had posterior predominant polymicrogyria with extension to the frontal lobe, and small groups of heterotopic neurons in the white matter. While the typical changes of polymicrogyria were not seen in the patient reported here, the frontal cortex was clearly abnormal, potentially consistent with the "delicate" form of polymicrogyria. Further, the blurred cortical–white matter border was also abnormal and would be consistent with heterotopic neurons in the white matter. No mutations were identified in XLF, LIGIV, or XRCC4, however. Additionally, the MRI images and the neurological features in this patient bore similarities to those previously seen in children with PNKP mutations (44). DNA-PK, as well as ataxia-telangiectasia mutated (ATM), phosphorylate PNKP (45), and PNKP functions during NHEJ, although it also functions in single-strand break repair. Further work is required to determine whether the overlapping clinical manifestations could have a common basis.

The DSB repair phenotypes are distinct from those of previously described RS-SCID patients. Cells from DNA ligase IV– and/or XLF-deficient patients have a hypomorphic phenotype that allows slow rejoining of all DSBs (8). Thus, they manifest a marked defect at early times after irradiation (e.g., 2–6 hours), but the defect becomes milder at later times, and finally all DSBs are rejoined. Artemis-defective cells show no defect at early times, since Artemis is dispensable for the fast DSB rejoining process, but a 10%–15%

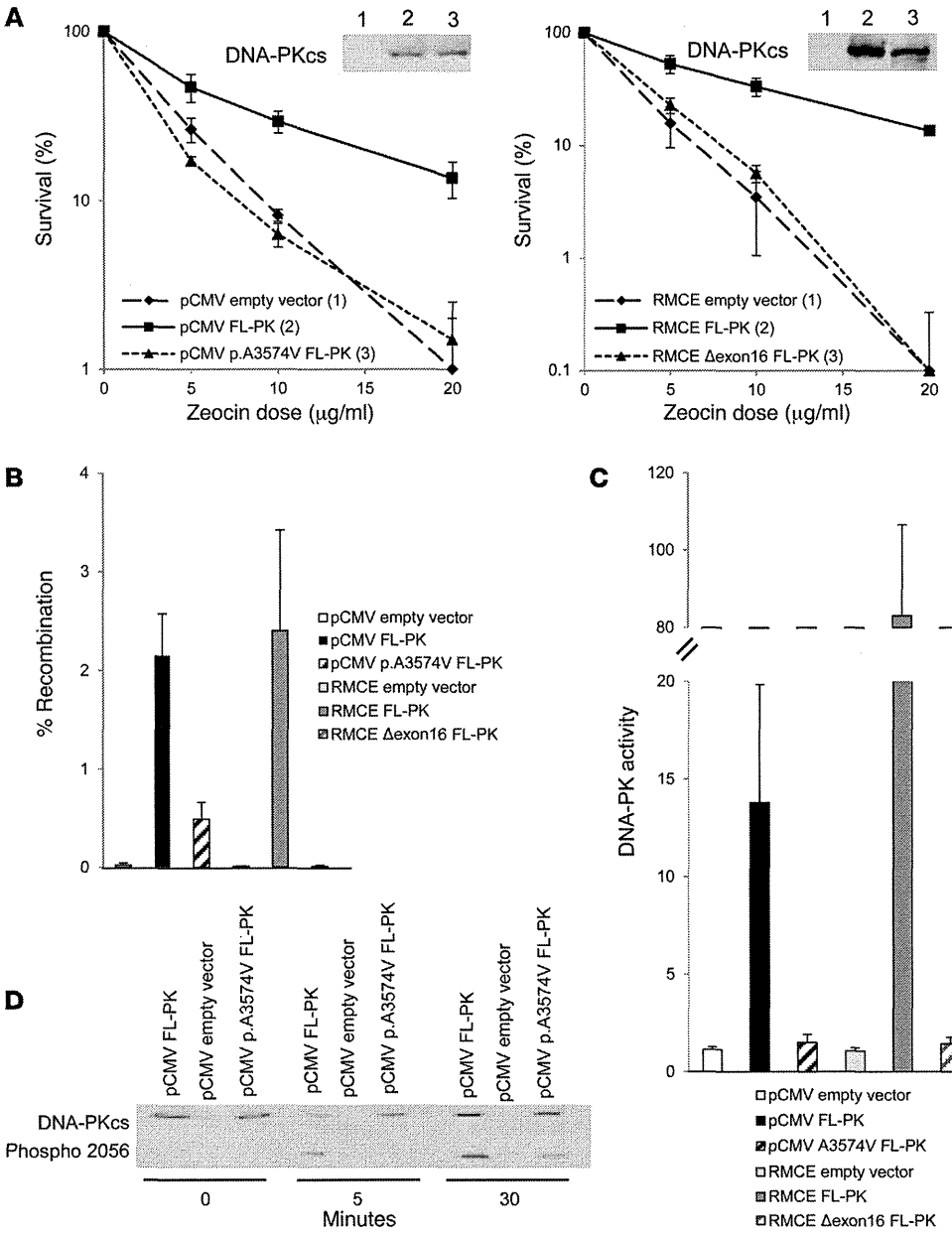

Figure 6
A3574V and exon 16–deleted DNA-PKcs impair DNA-PKcs kinase activity and DNA-PKcs function in the response to DNA damage and during V(D)J recombination. (**A**) Full-length, A3574V, or exon 16–deleted DNA-PKcs or empty vector was transiently transfected into DNA-PKcs–defective hamster V3 cells. 48 hours after transfection, cells were exposed to zeocin as indicated, and survival was estimated 7 days later. Expression of DNA-PKcs following Western blotting is also shown. Note that the exon 16–deleted DNA-PKcs cDNA was cloned into a distinct vector (RMCE) compared with A3574V DNA-PKcs cDNA (pCMV); the former is an improved vector for large inserts and was used in later studies. Survival analyses using these 2 vectors are presented separately. (**B**) Estimated percent recombination of coding junctions in V3 cells after expression of full-length, A3574V, or exon 16–deleted DNA-PKcs or empty vector together with plasmids encoding the RAG recombinases and a recombination substrate that assesses coding end-joining. (**C** and **D**) Estimation of DNA-PK activity in whole cell extracts from V3 cells expressing full-length, A3574V, or exon 16–deleted DNA-PKcs or empty vector. DNA-PK was extracted using DNA–cellulose beads, and activity was assessed using a biotinylated p53 peptide as a substrate (**C**) or by examining autophosphorylation after Western blotting and analysis using DNA-PKcs or phospho-2056–DNA-PKcs antibodies (**D**).

subfraction of DSBs remain unrejoined for prolonged times (8). The patient cells, in contrast, had a defect at early times after IR, although this was milder compared with DNA ligase IV–deficient cells; however, at later times, the defect remained marked and similar to that observed in Artemis-defective cells. Thus, patient cells cannot be described as being more or less defective than those of LIGIV syndrome patients — rather, the phenotype is distinct. The repair deficiency in patient cells appears less severe than that observed after treatment with DNA-PKi, potentially attributable to residual DNA-PK activity. Indeed, our functional analysis provides evidence that the change in the maternal allele (p.A3574V) confers low but detectable residual activity, predicting a hypomorphic phenotype. Nonetheless, despite residual activity, unrepaired DSBs were detectable at 8 days after 3 Gy in patient cells, which suggests that the slow component of DSB repair is almost fully inhibited. These findings are consistent with the notion that the different processes in which DNA-PKcs functions — e.g., fast versus slow DSB repair and V(D)J recombination — have different requirements for DNA-PK activity, and that the slow DSB repair process is dramatically affected by low DNA-PKcs activity.

In mice, loss of DNA ligase IV or XRCC4, both essential NHEJ proteins, is embryonic lethal, with marked apoptosis in the embryonic neuronal cells (11, 12). In humans, LIGIV syndrome and XLF-deficient patients, who harbor hypomorphic mutations in DNA ligase IV and XLF, respectively, display growth delay and microcephaly at birth, but the effect is not progressive postnatally (20, 21). A mouse model for LIGIV syndrome, *LigIV*^{Y288C}, which, like LIGIV syndrome patients, has a hypomorphic mutation in DNA ligase IV, also shows delayed growth, a small head, and elevated apoptosis in the embryonic neuronal stem cells (22, 46). As in

Table 1
Coding joints mediated by WT and A3574V DNA-PKcs

DNA-PKcs	Sequences	bp deletion		Junction change frequency		
	(*n*)	Mean	Median	Complete ends	P nt insertions	Short sequence homologies
WT	40	5.8	5.5	31% (25 of 80)	12% (3 of 25)	63% (25 of 40)
A3574V	55	4.3	4	34% (37 of 110)	35% (13 of 37)	36% (20 of 55)

Full-length WT and mutant A3574V DNA-PKcs cDNA was transfected into V3 cells, followed by transfection of plasmids encompassing coding junctions and the RAG1/2 nucleases. 48 hours after transfection, PCR amplification was carried out using primers that allow amplification of the rejoined coding junctions. Individual clones were sequenced. The changes observed at the junctions were similar following expression of WT and A3574V DNA-PKcs.

humans, the effect is not progressive postnatally. These findings suggest that there is a stringent requirement for the NHEJ ligation complex during embryonic neuronal development in mice and humans. Additionally, Ku-defective mice are viable, but display impaired embryonic neurogenesis (10, 47). In contrast, the animal models for DNA-PKcs loss (mice, dogs, and horses) have no evident neurological phenotype, despite having no detectable residual DNA-PKcs function (14–16, 47). Thus, the marked neuronal abnormalities in patient NM720 were completely unexpected based on findings from these animal models. Indeed, they showed not only that there is a stringent requirement for DNA-PKcs during embryonic neuronal development in humans, but that DNA-PKcs is also required postnatally.

At least 3 possible models underlying this marked clinical impact can be considered: (a) there is a more stringent requirement for DNA-PKcs for NHEJ in humans; (b) the clinical features arise from a non-NHEJ function of DNA-PKcs in humans, such as a role in telomere maintenance; or (c) there is a greater requirement for DSB repair during neuronal embryogenesis in humans. We and others have observed that mice and humans have a similar requirement for each NHEJ protein for DSB repair (8, 22). In both mouse and human cells, loss or inhibition of DNA-PKcs has a modest effect on the fast DSB repair component, but dramatically impairs the slow process (Figure 3). One explanation for residual DSB rejoining in the absence of DNA-PKcs is that an alternative form of end-joining can occur, whereas loss of DNA ligase IV results in almost complete loss of NHEJ in G0 phase mouse and human cells (48). Importantly, however, these requirements and alternative processes appear to function at similar levels in mice and in human cells (48); thus, the first possibility appears unlikely. The DNA-PK complex has also been shown to function in telomere maintenance, with this function being more important in humans than in mice (26, 28, 29, 49). However, if the clinical effect was predominantly due to telomere shortening, one might expect developmental defects in many tissues and cell types. Furthermore, since neurons are predominantly nonreplicating, the postnatal impact cannot readily be attributed to telomere shortening. An alternative possibility is that DNA-PK activity has a distinct role in the brain, potentially activating a response distinct to its role in DSB repair or activating a response that enhances survival to endogenously arising DSBs. However, although these possibilities cannot be eliminated, we favor the explanation that the clinical features are caused predominantly by the DSB repair defect and that neuronal development and maintenance in humans places a high demand on DSB repair capacity. The lack of a postnatal effect in LIGIV syndrome or XLF-deficient patients could be a consequence of their hypomorphic mutational changes.

Importantly, a distinguishing characteristic of NHEJ in primates versus all other vertebrates is remarkably high expression levels of all 3 DNA-PK component polypeptides. Indeed, DNA-PK protein and enzymatic activity is approximately 50-fold higher in human versus mouse cells (16, 50). This, however, does not affect DSB repair rates or radioresistance, which, as discussed above, are similar in rodents and humans. DNA-PK avidly binds to DSB ends, preventing their resection by exonucleases. Examination of DNA-PK dosage in cell line models has suggested that there is an inverse correlation between DNA-PKcs expression and the use of homologous recombination (HR), an alternative process of DSB repair (30). Consistent with this model, Hendrickson and colleagues have observed that loss of telomeres in Ku- or DNA-PKcs–deficient cells is mediated by HR and is dosage dependent (e.g., haplodeficient cells have a modest telomere loss phenotype; refs. 28, 29). Similarly, targeting efficiency, which is mediated by HR, is increased in a dose-dependent manner (51). We have suggested that differing requirements for DNA-PK levels in humans may reflect a more stringent requirement to regulate HR at hyper-recombinogenic genomic regions (30, 52). Thus, the high expression of DNA-PK in primates may suggest a unique necessity to restrain HR or other DSB repair pathways, which may be particularly important during neuronal development. In this context, it is notable that our analysis of *LigIV*^{Y288C} embryos revealed that significant levels of DSBs arise in the embryonic neuronal stem and early progenitor cells in a manner temporally related to the stage of rapid replication (22). Although previous studies have suggested that HR repairs replication-associated DSBs, DNA ligase IV is clearly required to repair the endogenous DSBs that arise in a manner associated with rapid replication. Importantly, the demand for efficient repair in this tissue is due not only to high DSB formation, but also to a low threshold for activating apoptosis from unrepaired DBSs (22). Thus, we propose that the high expression of DNA-PK proteins in primates is due, at least in part, to ensure efficient repair by NHEJ rather than HR during neuronal development. The embryonic neuronal stem and early progenitor cells may be particularly vulnerable to DNA-PKcs loss due to the high frequency of S/G2 phase cells, the cell cycle phase where HR functions, and where resection, the initiating step of HR, occurs avidly.

In summary, we provide the first identification of a patient with a profound defect in DNA-PKcs levels and activity. In addition to the expected SCID phenotype, the patient showed dramatically impaired neurological development and progressive brain atrophy, which was not anticipated based on animal models. Our findings suggest that high expression of DNA-PK component proteins in primates is required, at least in part, to ensure efficient embryonic neuronal development, which we postulate might be necessary to avoid DSB repair by HR.